Some Properties of the Higher-Order Images Reconstructed from Grating-Like Acoustical Holograms and their Applications for Multiplexing and Multi-Color Acoustical Holography*

Yoshinao AOKI**

(Received April 30, 1969)

Abstract

In this paper grating-like acoustical holograms are constructed by scanning the acoustical fields with a microphone. The optical reconstruction of image is conducted using laser light and the higher-order images were observed. The grating-like acoustical holograms were constructed by a Gabor's coherent background method, a two-beam interference method and an electronic reference method. The resulting higher-order images reconstructed from these holograms were discussed. Some properties of the higher-order images, contrast enhancement and contrast inversion, were analyzed from a point of non-linearity of the hologram recording system and the property of the grating.

For the applications of grating-like acoustical holograms, a space division multiplexing acoustical holography and a multi-color acoustical holography were proposed. An experiment to construct space divison multiplexing acoustical holograms was conducted, where information of different objects was recorded in a single grating-like acoustical hologram by scanning with a microphone. As a preliminary experiment to reconstruct a multi-color image from acoustical holograms, an experiment to reconstruct a single-color image from a grating-like acoustical hologram was conducted.

Contents

Abstract 249
1. Introduction 250
2. Some properties of the Higher-Order Images Reconstructed from Grating-Like Acoustical Holograms 251
2.1 Construction of Grating-Like Acoustical Holograms and Optical Reconstruction of the Higher-Order Images 251
2.2 Contrast Enhancement of the Higher-Order Images 257
2.3 Contrast Inversion of the Higher-Order Images 260
2.4 Higher-Order Images Reconstructed from Acoustical Holograms by a Two-Beam Interference Method 264

* This paper was presented at the Second International Symposium on Acoustical Holography at Douglas Advanced Research Laboratories, Huntington Beach, California, on March 6, 7, 1969.

** Department of Electronic Engineering, Faculty of Engineering, Hokkaido University, Sapporo, Japan.

2.5 Higher-Order Images Reconstructed from Acoustical Holograms by an Electronic Reference Method 270
3. Space Division Multiplexing Acoustical Holography 273
3.1 Theory 273
3.2 Experiment 275
4. Multi-Color Acoustical Holography 278
4.1 Theory 278
4.2 Preliminary Experiment 283
5. Conclusion 284
Acknowledgment 284
References 285

1. Introduction

In long-wavelength holographies such as sound (or ultrasonic) wave holography[1)-16)] and radio wave holography,[17)-23)] holograms are constructed by scanning the wave fields with a receiver (or detector). In long-wavelength holographies the scanning technique is inevitable except for some hologram-recording techniques inasmuch as the film sensors[2),23)] or other direct hologram-recording apparatus[1),13),14)] have not been sufficiently developed for these waves and the wave fields of the hologram plane are generally too large to be recorded on a sheet of film sensors, even if the film sensors for these waves are developed. Although it is physically possible to arrange two-dimensional arrays of receivers, each of which with an amplifier and a display element (for example, a lamp), it would be difficult from an economical point of view to arrange the arrays as closely as compared with the film sensors. Therefore two-dimensional arrays are arranged with suitable sampling periods on the hologram plane to obtain sufficient information for image reconstruction, where the amplification and display of hologram signals are done with an amplifier and a disply apparatus in such a way that mechanical or electronical scanning of the signals from the arrays of receivers is necessary. Usually a receiver scans the wave fields mechanically because this technique is simpler and less expensive than that of arrays of receivers.

The scanning (mechanical or electronical) is a technique to decompose two-dimensional spatial hologram information to one-dimensional temporal information and this technique provides some advantages in that we can use electronic components, circuits and systems, including electronic computers, for electronic measurement, transmission and information processing of hologram signals. In the scanning-type holography it is desirable to scan the wave fields as closely as possible but it is limited by the characteristics of the receiver which has a finit aperture and by the time required to construct hologram, etc. Therefore, in a simple case, the wave fields are scanned with suitable scanning periods such as used in television scanning and a grating-like hologram is constructed. The grating-like hologram recontructs higher-order images in the optical reconstruction process. These images resemble the images reconstructed from holograms by a two-beam interference method, but they differ in that an effective separation of

the true and conjugate images from the grating-like hologram can not be obtained whereas the true and conjugate images are separated in the two-beam interference holography. The grating-like hologram, however, has some advantageous properties and certain applications using these properties are available. In this paper theoretical and experimental analyses are made on the higher-order images reconstructed from grating-like acoustical holograms. Further applications of the grating-like holograms for a space division multiplexing acoustical holography and a multi-color acoustical holography are discussed.

2. Some Properties of the Higher-Order Images Reconstructed from Grating-Like Acoustical Holograms

2.1 Construction of grating-like acoustical holograms and optical reconstruction of the higher-order images

In the theroretical treatment of an imaging system, including the holographic system, the matrix method is convenient and this method was used to analyze the images reconstructed from the acoustical hologram in this paper. The matrix equations of ray-translation through a free space with a distance z (see Fig. 1) and a convex lens with a focal length F (see Fig. 2) are as follows,

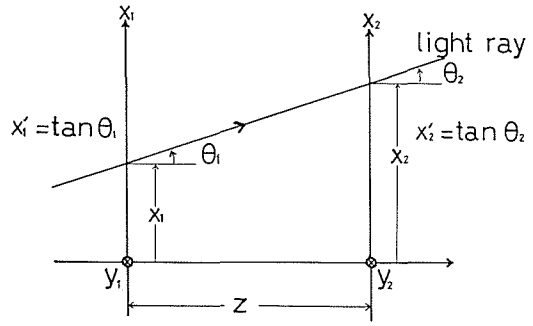

Fig. 1. Free space with distance Z.

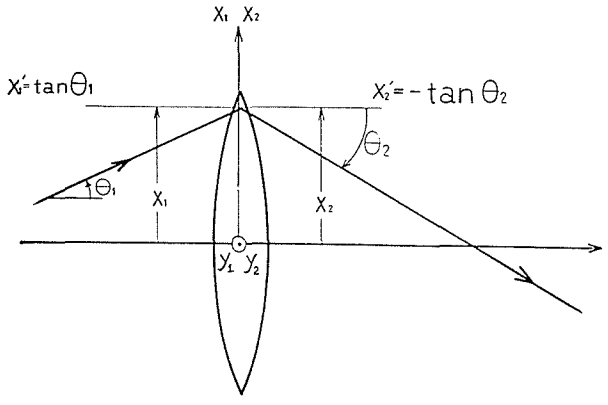

Fig. 2. Convex lens with focal length F.

$$\begin{bmatrix} x_2 \\ x_2' \end{bmatrix} = \begin{bmatrix} 1 & z \\ 0 & 1 \end{bmatrix} \begin{bmatrix} x_1 \\ x_1' \end{bmatrix} \tag{1}$$

$$\begin{bmatrix} x_2 \\ x_2' \end{bmatrix} = \begin{bmatrix} 1 & 0 \\ -\dfrac{1}{F} & 1 \end{bmatrix} \begin{bmatrix} x_1 \\ x_1' \end{bmatrix} \tag{2}$$

where x_1 and x_2 are the ray positions and x_1' and x_2' are the ray slopes. The subscripts 1 and 2 denote the coordinates on the entrance plane and exit plane of the free space and convex lens, respectively. The same matrix representation can be written for the y coordinate.

Now we assume that a Gabor-type[24] acoustical hologram is constructed in the arrangement as shown in Fig. 3 where Λ is the wavelength of the sound-wave, b and o are the background illumination and object sound-waves, (x_i, z_i)

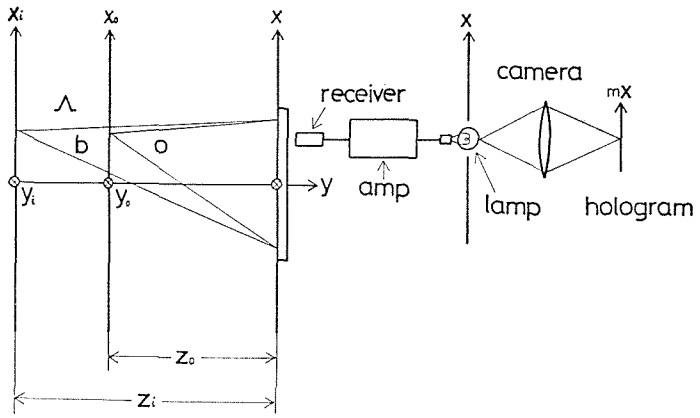

Fig. 3. Arrangement for constructing Gabor-type acoustical holograms.

and (x_0, z_0) are the coordinates of the sound-wave source and object, respectively, and m is the reduction rate of the hologram. We assume that an acoustical hologram is recorded by square-law detection and the hologram H is expressed as follows,

$$H = (b+o)(b+o)^* = |b|^2 + |o|^2 + b^*o + bo^* \tag{3}$$

where the terms b^*o and bo^* reconstruct the true and conjugate images. The matrix equation of ray-translation by the hologram concerning the terms b^*o and bo^* of Eq. (3) is expressed as follows,[11]

$$\begin{bmatrix} x_2 \\ x_2' \end{bmatrix} = \begin{bmatrix} 1 & 0 \\ \pm\dfrac{m^2}{\mu}\left(\dfrac{1}{z_0} - \dfrac{1}{z_i}\right) & 1 \end{bmatrix} \begin{bmatrix} x_1 \\ x_1' \end{bmatrix} + \begin{bmatrix} 0 \\ \mp\dfrac{m}{\mu}\left(\dfrac{x_0}{z_0} - \dfrac{x_i}{z_i}\right) \end{bmatrix} \tag{4}$$

where $\mu(=\Lambda/\lambda$; λ the wavelength of light in the optical reconstruction process) is a wavelength ratio of the sound-wave to the coherent light. The upper and lower signs of Eq. (4) correspond to the true and conjugate images, respectively,

and these signs are to be taken throughout.

In Fig. 3, a receiver scans the acoustic fields along the y coordinate with a suitable sampling period with respect to the x coordinate in such a way that a grating-like acoustical hologram is constructed. For simplification of the analysis we express the scanning of the receiver by the function $f(x)$ as shown in Fig. 4, where the receiver scans the acoustic fields at $f(x)=1$ with a scanning period d. The function $f(x)$ is expressed as follows,

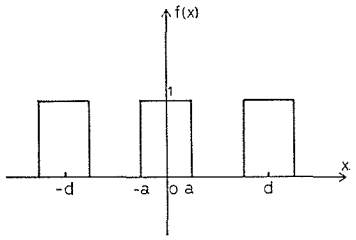

Fig. 4. Scanning lines of a receiver.

$$f(x)=\frac{2a}{d}\left[1+2\sum_{n=1}^{\infty}\frac{\sin(2\pi na\nu)}{2\pi na\nu}\cos(2\pi n\nu x)\right] \tag{5}$$

where $\nu\left(=\frac{1}{d}\right)$ is a fundamental spatial frequency of the function. The scanning lines shown in Fig. 4 act as a diffraction grating in the optical reconstruction process. This diffraction grating is represented for the n-th order diffracted waves by the following matrix equation,

$$\begin{bmatrix}x_2\\x_2'\end{bmatrix}=\begin{bmatrix}1&0\\0&1\end{bmatrix}\begin{bmatrix}x_1\\x_1'\end{bmatrix}+\begin{bmatrix}0\\\pm\lambda mn\nu_0\end{bmatrix} \tag{6}$$

where ν_0 is a fundamental spatial frequency of the grating and m is the reduction rate of the grating of Fig. 4.

Now we reconstruct images from the acoustical hologram of Eq. (4) with the grating of Eq. (6) to apply the collimated laser light as shown in Fig. 5. The ray translation from the entrance plane of the grating-like hologram to the image plane is obtained by the cascade product of the matrices of the free space (Eq. (1)), a diffraction grating (Eq. (6)) and the hologram (Eq. (4)) as shown in Eq. (7).

$$\begin{bmatrix}x_2\\x_2'\end{bmatrix}=\begin{bmatrix}1&z\\0&1\end{bmatrix}\left\{\begin{bmatrix}1&0\\\pm\frac{m^2}{\mu}\left(\frac{1}{z_0}-\frac{1}{z_i}\right)&1\end{bmatrix}\begin{bmatrix}x_1\\0\end{bmatrix}+\begin{bmatrix}0\\\mp\frac{m}{\mu}\left(\frac{x_0}{z_0}-\frac{x_i}{z_i}\right)\end{bmatrix}+\begin{bmatrix}0\\(\pm)\lambda mn\nu_0\end{bmatrix}\right\} \tag{7}$$

$$=\begin{bmatrix}1\pm z\frac{m^2}{\mu}\left(\frac{1}{z_0}-\frac{1}{z_i}\right)&z\\\pm\frac{m^2}{\mu}\left(\frac{1}{z_0}-\frac{1}{z_i}\right)&1\end{bmatrix}\begin{bmatrix}x_1\\0\end{bmatrix}+\begin{bmatrix}\mp z\frac{m}{\mu}\left(\frac{x_0}{z_0}-\frac{x_i}{z_i}\right)(\pm)\lambda mn\nu_0 z\\\mp\frac{m}{\mu}\left(\frac{x_0}{z_0}-\frac{x_i}{z_i}\right)(\pm)\lambda mn\nu_0\end{bmatrix}$$

where the variables x_1, x_1' $(=0)$ and x_2, x_2' express the rays at the entrance plane of the hologram and the image plane, respectively. The reconstruction condition of images obtainable from the matrix element of Eq. (7) under the condition that the image coordinate x_2 must be determined independently of the coordinate x_1 of rays at the hologram plane, and is given by,

$$\frac{1}{z_{(\mp)}} = \mp \frac{m^2}{\mu}\left(\frac{1}{z_0} - \frac{1}{z_i}\right). \tag{8}$$

Using Eq. (8), we obtain the coordinate x_2 of the reconstructed images from Eq. (7) which is as follows,

$$x_2 = \frac{\mu}{m^2} \frac{1}{\left(\frac{1}{z_0} - \frac{1}{z_i}\right)} \left[\frac{m}{\mu}\left(\frac{x_0}{z_0} - \frac{x_i}{z_i}\right)(\mp)\lambda m n \nu_0\right]. \tag{9}$$

In Eqs. 8 and 9 the upper and lower signs represent the true and conjugate images, respectively, and these signs are to be taken throughout the study except for the signs in parenthesis in Eq. (9). From Eq. (9) we see that higher-order images appear[16),25)] by the scanning lines as shown in Fig. 5.

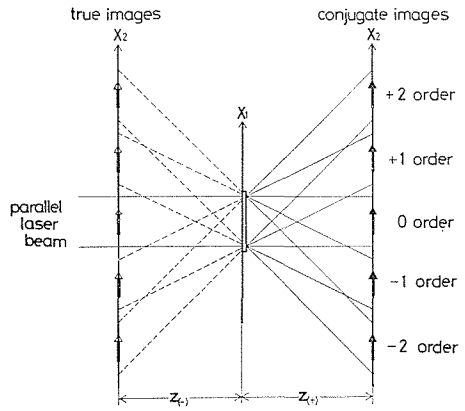

Fig. 5. Reconstructed higher-order true and conjugate images from a grating-like acoustical hologram.

The acoustical holograms are constructed in the experimental arrangement as shown in Fig. 6. A tweeter radiates sound-waves to illuminate objects. The objects are letters made of aluminum plates. At the hologram plane a dynamic microphone (with an aperture of about 2 cm diameter) scans the acoustic fields of about 2 m × 2 m. The scanning of the microphone is done mechanically and auto-

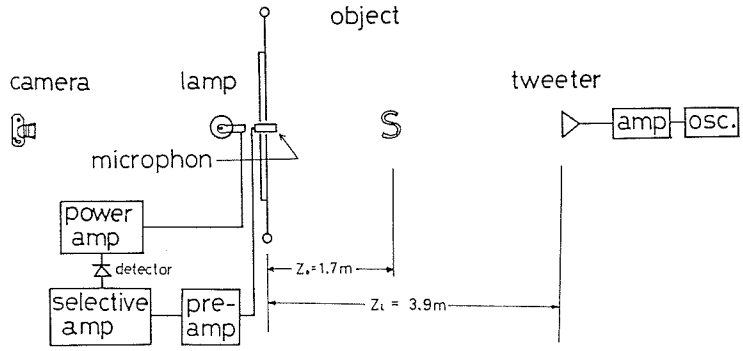

Fig. 6. Experimental arrangement for constructing acoustical holograms.

matically using vertical and horizontal motors and an electronic control circuit. The output signals from the microphone are amplified by a pre-amplifier, a selective amplifier and a power amplifier. These amplified signals light a lamp fixed to the microphone and a camera records the light intensity distribution converted from the acoustical field as an acoustical hologram.

Acoustical holograms are constructed for various scanning periods d of Fig. 4. The obtained holograms of an object of the letter S (18 cm × 28 cm, with 3.5 cm line-width) of Fig. 7 are shown in Fig. 8 where the scanning periods are

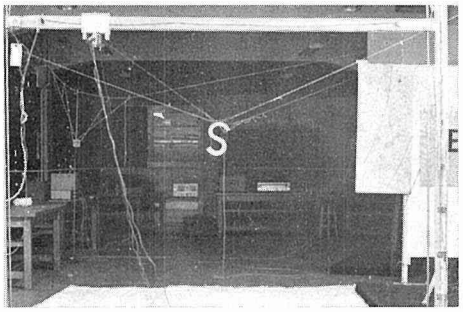

Fig. 7. Object (the letter S) and experimental equipment.

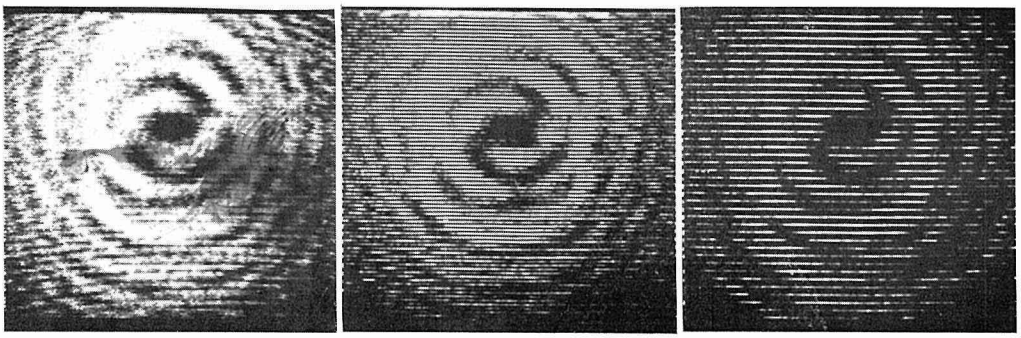

Fig. 8. Acoustical holograms constructed in the experimental arrangement of Fig. 6. The scanning periods of the microphone are $d=1$ cm (a), $d=2$ cm (b), and $d=4$ cm (c).

$d=1$ cm (Fig. 8-a), $d=2$ cm (Fig. 8-b) and $d=4$ cm (Fig. 8-c). The distance z_0 from the object to the microphone is 1.7 m and z_i from the tweeter to the microphone is 3.9 m. The frequency of the sound-wave is chosen as 15 kHz. As may be seen the grating-like holograms are constructed in Fig. 8.

The optical reconstruction of images are conducted in the optical system as shown in Fig. 9 where laser light of 6328 Å wavelength is used. The photograph of the optical system of Fig. 9 is shown in Fig. 10. In the optical reconstruction of an acoustical hologram the wavelength ratio is large. For example the wavelength Λ of the sound-wave is 2.3 cm (at the frequency of 15 kHz in air) and the wavelength λ of laser light is 0.63 μ, resulting in the wavelength ratio $\mu = \frac{2.3}{0.63\times10^{-4}} = 3.7\times10^{4}$. This fact shows that the acoustical hologram must be

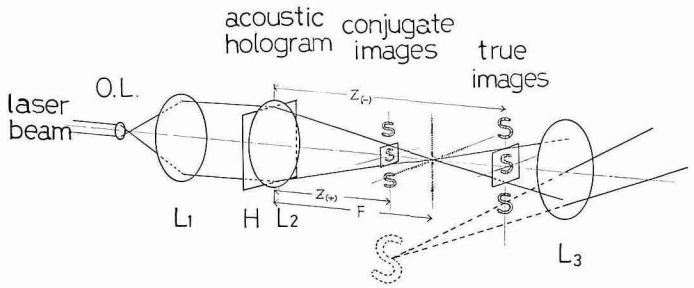

Fig. 9. Optical system for reconstructing images from reduced acoustical holograms.

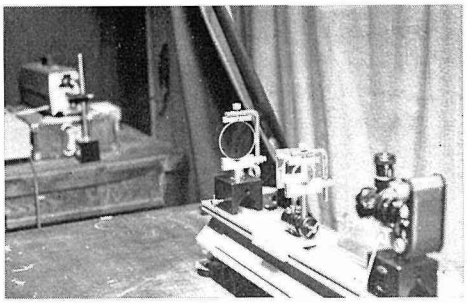

Fig. 10. Photograph of the optical system of Fig. 9.

reduced for the optical reconstruction in a laboratory system according to Eq. 8. In this experiment the acoustical holograms are reduced to 4 mm × 4 mm and the collimated laser beam produced by the objective O.L. and a collimating lens L_1 is applied to the reduced hologram as shown in Fig. 9. As the reconstructed images are small because of the smaller size of the hologram, the real images of the true and conjugate images are reproduced by lens L_2 and the magnified images by lens L_3 are observed.

In the optical system of Fig. 9 the translation of rays from the entrance plane of the hologram to the image plane is obtained by the cascade product of the matrices of the free space, a convex lens with focal length F and the grating-like acoustical hologram, as shown by,

$$\begin{bmatrix} x_2 \\ x_2' \end{bmatrix} = \begin{bmatrix} 1 & z \\ 0 & 1 \end{bmatrix} \left[\begin{bmatrix} 1 & 0 \\ -\frac{1}{F} & 1 \end{bmatrix} \left(\begin{bmatrix} 1 & 0 \\ \pm\frac{m^2}{\mu}\left(\frac{1}{z_0}-\frac{1}{z_i}\right) & 1 \end{bmatrix} \begin{bmatrix} x_1 \\ 0 \end{bmatrix} + \begin{bmatrix} 0 \\ \mp\frac{m}{\mu}\left(\frac{x_0}{z_0}-\frac{x_i}{z_i}\right)(\pm)\lambda m n \nu_0 \end{bmatrix} \right) \right]$$

$$= \begin{bmatrix} 1-\frac{z}{F} \pm z\frac{m^2}{\mu}\left(\frac{1}{z_0}-\frac{1}{z_i}\right) & z \\ -\frac{1}{F} \pm \frac{m^2}{\mu}\left(\frac{1}{z_i}-\frac{1}{z_i}\right) & 1 \end{bmatrix} \begin{bmatrix} x_1 \\ 0 \end{bmatrix} + \begin{bmatrix} \mp z\frac{m}{\mu}\left(\frac{x_0}{z_0}-\frac{x_i}{z_i}\right)(\pm)\lambda m n \nu_0 z \\ \mp\frac{m}{\mu}\left(\frac{x_0}{z_0}-\frac{x_i}{z_i}\right)(\pm)\lambda m n \nu_0 \end{bmatrix}. \quad (10)$$

From the matrix element of Eq. (10), the positions $z_{(-)}$ and $z_{(+)}$ of the true and conjugate image planes are obtained and are as follows,

$$\frac{1}{z_{(\mp)}} = \frac{1}{F} \mp \frac{m^2}{\mu}\left(\frac{1}{z_0} - \frac{1}{z_i}\right). \tag{11}$$

The coordinates of images are obtained using Eq. (11),

$$x_{2(\mp)} = \mp z_{(\mp)}\left[\frac{m}{\mu}\left(\frac{x_0}{z_0} - \frac{x_i}{z_i}\right)(\pm)\lambda m n \nu_0\right] \tag{12}$$

where the negative and positive signs represent the coordinates of the true and conjugate images. Equations (11) and (12) coincide with Eqs. (8) and (9), as $F \to \infty$ in Eqs. (11) and (12), respectively. From Eq. (11) we see $z_{(-)} > F > z_{(+)} > 0$ and that the true and conjugate images are reconstructed as shown in Fig. 9. From Eq. (12) we see that the true image is reconstructed in reverse with respect to the conjugate image and higher-order images make their appearance.

The reconstructed true and conjugate images are observed in the optical system of Fig. 9. These images are reconstructed according to the relations of

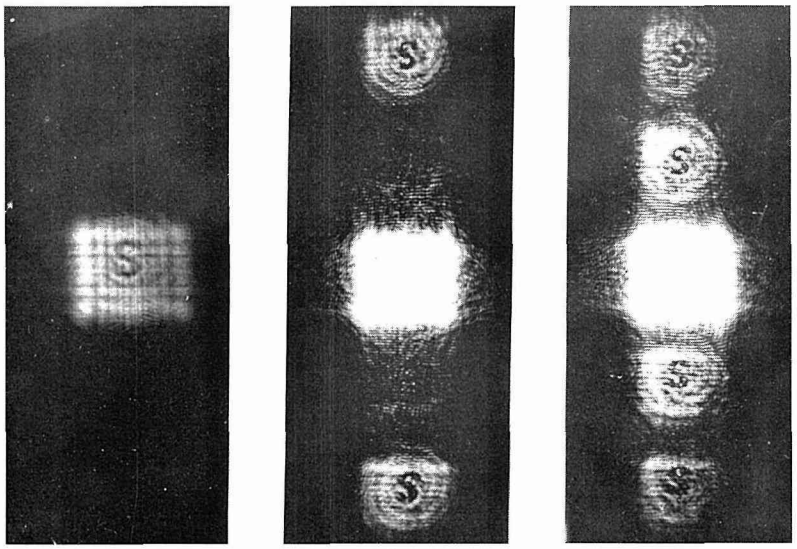

Fig. 11. Reconstructed cojugate images from the holograms of Fig. 8, where a, b, and c are the images from Fig. 8-a, b, and c, respectively.

Eqs. (11) and (12). The reconstructed conjugate images from the hologram of Fig. 8 are shown in Fig. 11-a, b, and c. In Fig. 11-a, only a zero-order image is reconstructed. While first-order images are reconstructed in Fig. 11-b and first and second-order images are reconstructed in Fig. 11-c where zero-order images disappear due to the strong background.

2.2 Contrast enhancement of higher-order images

In the process of constructing an acoustical hologram, the acoustical fields are converted to electrical signals and successively to light signals and are recorded finally on a film as a hologram. Therefore the recorded acoustical fields are

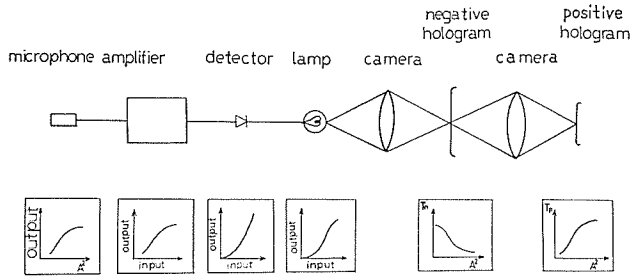

Fig. 12. Non-linear characteristics of each component of the acoustical-hologram recording system.

subjected to the characteristics of a microphone, an amplifier, a detector, a lamp and films as shown in Fig. 12. The characteristics of output signals versus input signals of each components of Fig. 12 are not always linear, in other words, the transparency of light amplitude of an acoustical hologram finally recorded on a film is not linearly proportional to the intensity of original acoustical fields at the hologram plane. This non-linearity has some effects on the reconstructed images. One of them is the contrast enhancement of the higher-order images and this effect appears in the reconstructed images of Fig. 11-b and c where the higher-order images show a higher contrast than the zero-order images disturbed by the background light.

To explain the contrast enhancement of the higher-order images, we assume the characteristic curve of light transparency T_p of the final positive hologram versus the intensity A^2 of the acoustical fields at the hologram plane as shown in Fig. 13 by the dotted curve. For simplicity of analysis, we approximate the dotted curve by solid lines and express the linear section of the curve of T_p versus A^2 by the following equation,

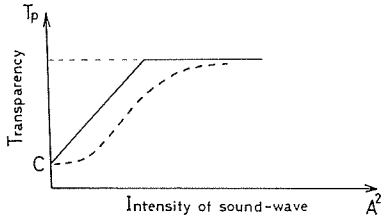

Fig. 13. Simplified characteristics of light transparency of a positive acoustical hologram versus the intensity of acoustical fields.

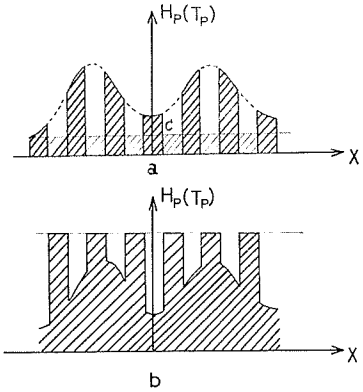

Fig. 14. Two types of grating-like acoustical holograms. In the hologram of a, $T_p=C$ at the unsampled hologram space, while in the hologram of b, $T_p=1$ at the unsampled hologram space.

$$T_p = C + K_p A^2 \tag{13}$$

where C and K_p are positive constants. We assume a grating-like hologram is constructed by the scanning of a microphone shown in Fig. 4 and a positive hologram is recorded under the charactersitics of Eq. (13). Figure 14-a shows a schematic figure of the positive hologram H_p where $T_p = C$ at the unsampled part. This positive hologram is expressed by,

$$\begin{aligned} H_p &= C + K_p f(|b|^2 + |o|^2 + b^*o + bo^*) \\ &= C + K_p f_0(|b|^2 + |o|^2 + b^*o + bo^*) \\ &\quad + K_p f_1(|b|^2 + |o|^2 + b^*o + bo^*) \end{aligned} \tag{14}$$

where f is the function of the scanning lines expressed by Eq. (5) and we consider only the zero-order term f_0 and first-order term f_1 of f. In the hologram of Eq. (14) the background term of the zero-order images is $C + K_p f_0(|b|^2 + |o|^2)$ while the background term of the first-order images is $K_p f_1(|b|^2 + |o|^2)$. This means the ratio of amplitude of the zero-order images to the background is smaller than that of the first-order images to the background and that the contrast enhancement occurs in higher-order images. Here the contrast enhancement of the higher-order images is explained as the saturation of the transparency at the low value part of A^2, where we describe the saturation effect by the constant C, simply as a convenience.

In contrast we assume that a grating-like acoustical hologram is constructed as shown in Fig. 14-b where the transparency of the hologram is made equal to unity at the unsampled space by some means. We assume that a positive hologram H_p of Fig. 14-b is recorded under the characteristics of Eq. (13) and we can express the hologram as follows,

$$\begin{aligned} H_p &= 1 - f + C + K_p f(|b|^2 + |o|^2 + b^*o + bo^*) \\ &= 1 - f_0 + C + K_p f_0(|b|^2 + |o|^2) + K_p f_0(b^*o + bo^*) \\ &\quad + f_1\left[-1 + K_p(|b|^2 + |o|^2) + K_p(b^*o + bo^*)\right]. \end{aligned} \tag{15}$$

In the hologram of Eq. (15), the background term concerning the zero-order images is $1 - f_0 + C + K_p f_0(|b|^2 + |o|^2)$ while the background term concerning the first-order images is $-f_1 + K_p f_1(|b|^2 + |o|^2)$. This means the intensity ratio of the image terms $K_p f_1(b^*o + bo^*)$ versus the background term of the first-order images is larger than that of the image term $K_p f_0(b^*o + bo^*)$ versus the background term of the zero-order images. As a result the contrast enhancement of the higher-order images occurs. The background term of the zero-order images is intensified when the bias term $|b|^2$ increases, while the background term of the first-order images is weakened when the bias term $|b|^2$ increases. This fact means that, when the saturation effect of the transparency at the high value part of A^2 occurs strongly, the bias term increases so that the contrast enhancement is emphasized in the first-order images.

An acoustical hologram as shown in Fig. 14-b is constructed in the experi-

mental arrangement of Fig. 6, where the conditions for constructing holograms are the same as those used in constructing the holograms of Fig. 8. The process through which the hologram is constructed is as follows; at the forward scanning of the microphone, the signals from the microphone are amplified and light a lamp, while at the backward scanning a constant signal with sufficient level to light the lamp brightly, is fed into the lamp instead of the signals from the microphone. The sufficiently exposed places of the film have a tranceparency of $T_p=1$ in the positive hologram and we can construct the hologram of Fig. 14-b in this process. The obtained hologram is shown in Fig. 15 where the scanning period d is 2 cm.

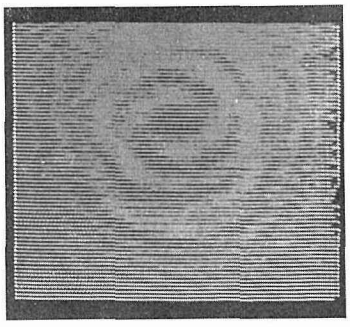

Fig. 15. Grating-like acoustical hologram of Fig. 14-b type.

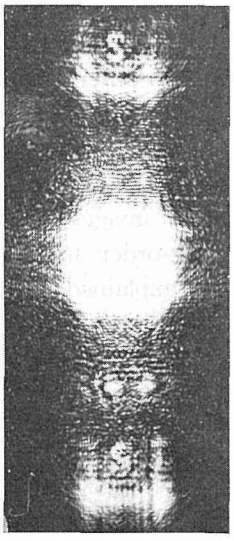

Fig. 16. Reconstructed first-order conjugate images from the hologram of Fig. 15.

The optical reconstruction of images is done in the experimental arrangement of Fig. 9. The obtained conjugate images are shown in Fig. 16 where the contrast enhancement of the higher-order images occurs. Comparing the higher-order images of Fig. 11 and Fig. 16, we see that the contrast inversion of the higher-order images occurs. This will be explained in the next section. The contrast enhancement is an important property of the higher-order images reconstructed from a grating-like hologram and it is useful for certain applications, for example space division multiplexing holography.

2.3 Contrast inversion of higher-order images

In the preceding section we discussed the higher-order images reconstructed from two types of grating-like holograms as shown in Fig. 14. In these images we observe the effects of not only contrast enhancement but also of contrast inversion as shown in Fig. 16. The higher-order images of Fig. 11 reconstructed from the grating-like hologram of Fig. 14-a type are dark images with a bright

background. In contrast the higher-order image of Fig. 16 reconstructed from the grating-like hologram of Fig. 14-b type are bright images with a dark background. We call the former images (reconstructed from Fig. 14-a) dark-contrast images or normal-contrast images whose contrast coincides with that of the original object which is an obstacle placed in the sound-wave background. We call the latter images (reconstructed from Fig. 14-b) bright-contrast images or inverse-contrast images because the contrast of the image is inverted against that of the object. Here the reason why the inverse-contrast images appear from the grating-like hologram of Fig. 14-b is explained from the signs of the background and image terms of the hologram. In the hologram of Eq. (14) the background terms are positive concerning both zero and first-order images and the reconstructed zero and first-order images are normal-contrast images in this case. In contrast in the hologram of Eq. (15) the background term $-1+K_p(|b|^2+|o|^2)$ concerning the first-order images is negative while the image terms retain the same sign as the image terms of Eq. (14). This means that background light concerning the first-order images undergoes a phase change of $e^{\pm i\pi}(=-1)$ while the light by image terms does no phase change, resulting in the inverse-contrast first-order images. Therefore, we can determine by checking the signs of both background and image terms, whether the reconstructed images are in normal-contrast or in inverse-contrast.

We discuss here the negative hologram H_n in addition to the positive holograms of Eqs. (14) and (15). We assume the characteristics of transparency T_n

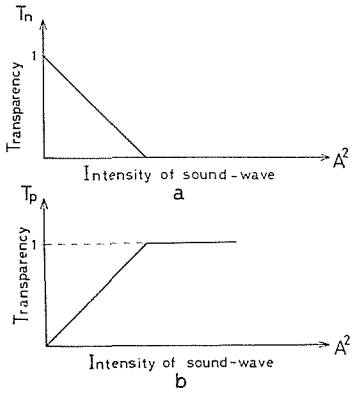

Fig. 17. Simplified characteristics of light transparency of a negative acoustical hologram (a) and a positive acoustical hologram (b) versus the intensity of acoustical fields.

and T_p of the negative and positive acoustical holograms versus the intensity A^2 of acoustical fields as shown in Fig. 17-a and b for simplicity of discussion. In Fig. 17 the linear parts of the characteristics is expressed by,

$$T_n = 1-K_nA^2 \tag{16}$$

$$T_p = K_pA^2 \tag{17}$$

where K_n and K_p are positive constants.

The negative hologram H_n and positive hologram H_p constructed by the two types of scanning of Fig. 14 are expressed using Eqs. (16) and (17) and are listed in Table 1. In this table positive and negative signs denote the sign of the background to the image terms as mentioned before so that the normal-contrast images are reconstructed for the positive sign and the inverse-contrast images are recon-

Table 1. Four types of grating-like acoustical holograms and their reconstructed images

	[I]	[II]	[III]	[IV]
	positive hologram	negative hologram	positive hologram	negative hologram
Representation of hologram	$H_p = K_p f_0(\|b\|^2 + \|o\|^2 + b^*o + bo^*)$ $+ K_p f_1(\|b\|^2 + \|o\|^2 + b^*o + bo^*)$	$H_n = 1 - K_n f_0(\|b\|^2 + \|o\|^2)$ $- K_n f_0(b^*o + bo^*)$ $- K_n f_1(\|b\|^2 + \|o\|^2 + b^*o + bo^*)$	$H_p = 1 - f_0 + K_p f_0(\|b\|^2 + \|o\|^2$ $+ b^*o + bo^*) - f_1$ $+ K_p f_1(\|b\|^2 + \|o\|^2 + b^*o + b^*o)$	$H_n = f_0 - K_n f_0(\|b\|^2 + \|o\|^2$ $- K_n f_0(b^*o + bo^*)$ $+ f_1 - K_n f_1(\|b\|^2 + \|o\|^2)$ $- K_n f_1(b^*o + bo^*)$
For zero-order image	+	−	+	−
For first-order image	+	+	−	−
Transparency of holograms	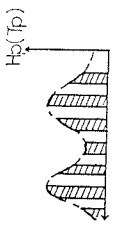 T-a	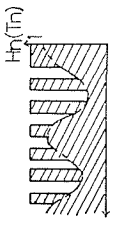 T-b	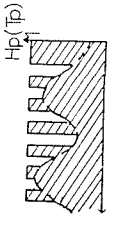 T-c	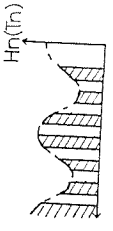 T-d
Reconstructed zero and first-order image	 T-1	 T-2	 T-3	 T-4

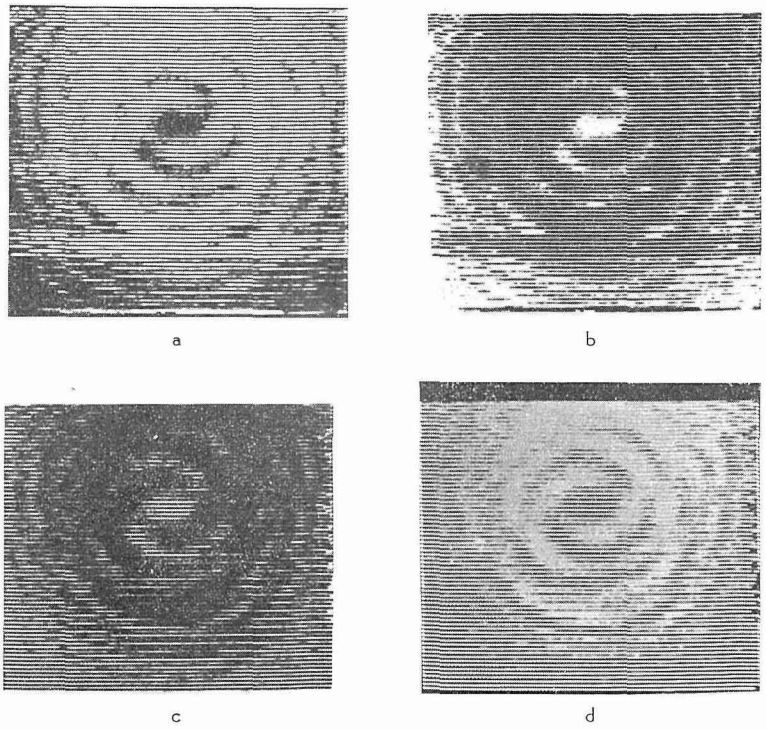

Fig. 18. Grating-like acoustical holograms, where a, b, c, and d correspond to the holograms of [I], [II], [III] and [IV] in Table 1, respectivery.

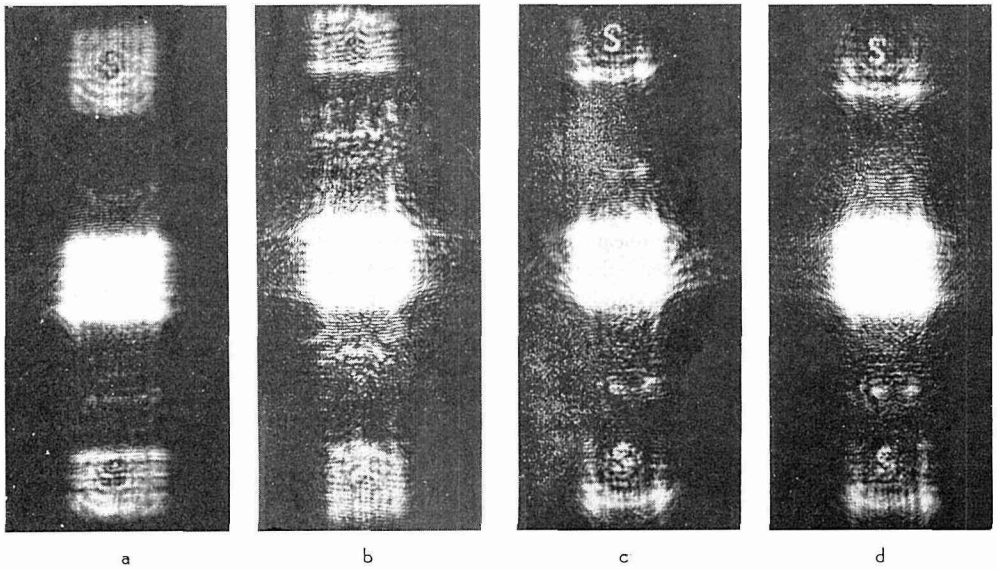

Fig. 19. Reconstructed first-order conjugate images from the holograms of Eig. 18, where a, b, c and d correspond to Fig. 18-a, b, c and d.

structed for the negative sign. In the middle columns the transparencies of the light of the grating-like holograms are drawn and in the lowest columns the reconstructed images are shown.

To verify the results of Table 1, four types of grating-like acoustical holograms shown in Table 1 were constructed. The obtained holograms are shown in Fig. 18-a~d which correspond to the holograms of [I], [II], [III], and [IV] in Table 1, respectively. The optical reconstruction of images was carried out in the optical system of Fig. 9 and the obtained reconstructed conjugate images are shown in Fig. 19-a~d. These reconstructed images verify the results of Table 1.

2.4 Higher-order images reconstructed from acoustical holograms by a two-beam interference method

In the preceding section we discussed Gabor-type acoustical holograms. In this section we analyze the acoustical hologram by a two-beam interference method which was developed by Leith and Upatnieks in optical holography.[26),27)] In a two-beam interference method, the acoustical holograms are constructed in the experimental arrangement of Fig. 20 where a reference acoustical wave is applied

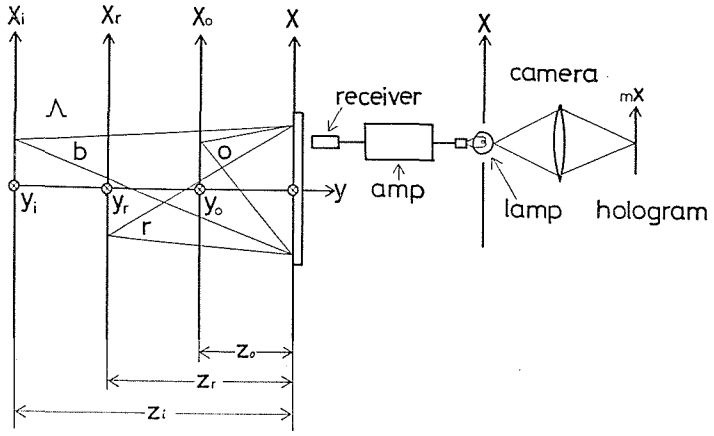

Fig. 20. Arrangement for constructing acoustical holograms by the two-beam interference method, where b, o and r represent the illumination sound-wave, object sound-wave and reference sound-wave, respectively.

to construct the hologram. We assume that an acoustical hologram by the two-beam interference method is recorded by square-law detection similar to the recordings of the Gabor-type hologram of Eq. (3) and the hologram is expressed as follows,

$$H=(b+r+o)(b+r+o)^*$$
$$=|b|^2+|r|^2+|o|^2+br^*+b^*r+b^*o+bo^*+r^*o+ro^*\,. \tag{18}$$

The sixth term b^*o and seventh term bo^* of the right hand side of Eq. (18) are similar to the third and fourth terms of the right hand side of Eq. (3) and

these terms reconstruct images similar to those of the Gabor-type hologram. The eighth term r^*o and nineth term ro^* of the right hand side of Eq. (18) reconstruct images separately from the bias beam. The matrix representation of the hologram of Eq. (18) concerning the image terms r^*o and ro^* are obtained to replace the coordinates (x_i, z_i) of the illumination sound-wave source by the coordinates (x_r, z_r) of the reference sound-wave source in Eq. (4),

$$\begin{bmatrix} x_2 \\ x_2' \end{bmatrix} = \begin{bmatrix} 1 & 0 \\ \pm\frac{m^2}{\mu}\left(\frac{1}{z_0}-\frac{1}{z_r}\right) & 1 \end{bmatrix}\begin{bmatrix} x_1 \\ x_1' \end{bmatrix} + \begin{bmatrix} 0 \\ \mp\frac{m}{\mu}\left(\frac{x_0}{z_0}-\frac{x_r}{z_r}\right) \end{bmatrix}$$

$$= \begin{bmatrix} 1 & 0 \\ \pm\frac{m^2}{\mu}\left(\frac{1}{z_0}-\frac{1}{z_i}+\frac{1}{z_c}\right) & 1 \end{bmatrix}\begin{bmatrix} x_1 \\ x_1' \end{bmatrix} + \begin{bmatrix} 0 \\ \mp\frac{m}{\mu}\left(\frac{x_0}{z_0}-\frac{x_i}{z_i}+\frac{x_c}{z_c}\right) \end{bmatrix} \quad (19)$$

where

$$\frac{1}{z_c} = \frac{1}{z_i} - \frac{1}{z_r}$$

$$\frac{x_c}{z_c} = \frac{x_i}{z_i} - \frac{x_r}{z_r}. \quad (20)$$

The coordinates (x_c, z_c) defined by Eq. (20) are the coordinates concerning the spatial carrier wave produced by the illumination wave b and the reference wave r. We can analyze the images reconstructed from an acoustical hologram by the two-beam interference method using Eq. (19).

Now we discuss the higher-order images reconstructed from the grating-like hologram by the two-beam interference method. For simplicity of analysis, we assume that the illumination and reference sound-waves are plane waves whose wavefronts are parallel to the y coordinate in Fig. 20, namely $1/z_c=0$ and $y_c/z_c=0$. This conditions means that the grating produced by the illumination wave b and the reference wave r runs along the y coordinate and only the x component of the spatial frequency of the grating exists. We assume that the hologram is constructed by scanning with a microphone along the x coordinate with the sampling frequency ν_0 with respect to y coordinate. The optical reconstruction of images is conducted from this grating-like hologram in the optical system of Fig. 9 and the ray translation from the hologram to the image plane is obtained by,

$$\begin{bmatrix} x_2 \\ x_2' \\ y_2 \\ y_2' \end{bmatrix} = \begin{bmatrix} 1 & z & 0 & 0 \\ 0 & 1 & 0 & 0 \\ 0 & 0 & 1 & z \\ 0 & 0 & 0 & 1 \end{bmatrix}\begin{bmatrix} 1 & 0 & 0 & 0 \\ -\frac{1}{F} & 1 & 0 & 0 \\ 0 & 1 & 0 & 0 \\ 0 & 0 & -\frac{1}{F} & 1 \end{bmatrix}\begin{bmatrix} 1 & 0 & 0 & 0 \\ \pm\frac{m^2}{\mu}\frac{1}{z_0} & 1 & 0 & 0 \\ 0 & 0 & 1 & 0 \\ 0 & 0 & \pm\frac{m^2}{\mu}\frac{1}{z_0} & 1 \end{bmatrix}\begin{bmatrix} x_1 \\ 0 \\ y_1 \\ 0 \end{bmatrix}$$

$$+\begin{bmatrix} 0 \\ \pm\frac{m}{\mu}\left(\frac{x_0}{z_0}-\frac{x_i}{z_i}+\frac{x_c}{z_c}\right) \\ 0 \\ \mp\frac{m}{\mu}\frac{y_0}{z_0}(\pm)\lambda mn\nu_0 \end{bmatrix}=\begin{bmatrix} 1-\frac{z}{F}\pm\frac{m^2}{\mu}\frac{z}{z_0} & z & 0 & 0 \\ -\frac{1}{F}\pm\frac{m^2}{\mu}\frac{1}{z_0} & 1 & 0 & 0 \\ 0 & 0 & 1-\frac{z}{F}\pm\frac{m^2}{\mu}\frac{z}{z_0} & z \\ 0 & 0 & -\frac{1}{F}\pm\frac{m^2}{\mu}\frac{1}{z_0} & 1 \end{bmatrix}\begin{bmatrix} x_1 \\ 0 \\ y_1 \\ 0 \end{bmatrix} \tag{21}$$

$$+\begin{bmatrix} \mp z\frac{m}{\mu}\left(\frac{x_0}{z_0}-\frac{x_i}{z_i}+\frac{x_c}{z_c}\right) \\ \mp\frac{m}{\mu}\left(\frac{x_0}{z_0}-\frac{x_i}{z_i}+\frac{x_c}{z_c}\right) \\ \mp z\frac{m}{\mu}\frac{y_0}{z_0}(\pm)\lambda mn\nu_0 z \\ \mp\frac{m}{\mu}\frac{y_0}{z_0}(\pm)\lambda mn\nu_0 \end{bmatrix}$$

where the matrices of the free space, a convex lens and a grating-like hologram are extended to two-dimentional forms and x_1, y_1 and $x_1'(=0)$, $y_1'(=0)$ are the positions and slopes of the rays on the entrance plane of the hologram and x_2, y_2 and x_2', y_2' are those of the rays on the image plane. The reconstruction condition is obtained from the matrix element of Eq. (21) as follows,

$$\frac{1}{z_{(\pm)}}=\frac{1}{F}\mp\frac{m^2}{\mu}\frac{1}{z_0}. \tag{22}$$

Equation (22) corresponds to Eq. (11).

Using Eq. (22) the coordinates of images are obtained as follows,

$$\begin{aligned} x_2&=\mp z_{(\mp)}\cdot\frac{m}{\mu}\left(\frac{x_0}{z_0}-\frac{x_i}{z_i}+\frac{x_c}{z_c}\right) \\ y_2&=\mp z_{(\mp)}\left[\frac{m}{\mu}\frac{y_0}{z_0}(\pm)\lambda mn\nu_0\right]. \end{aligned} \tag{23}$$

In Eqs. (22) and (23) the negative and positive signs correspond to the true and conjugate images, respectively. Equation (23) shows that the true and conjugate images are reconstructed apart from the y_2 axis by $\mp\frac{m}{\mu}\frac{x_c}{z_c}z_{(\mp)}$ and the higher-order images are reconstructed apart from the x_2 axis by $\pm\lambda mn\nu_0 z_{(\mp)}$ in the image plane as shown in Fig. 21 where the zero and first-order true images are drawn.

The acoustical holograms by the two-beam interference method are constructed in the experimental arrangement of Fig. 22. First the reference wave is cut off and only the illumination sound-wave is applied to the object (a letter X made of an aluminum plate) and a hologram is constructed with a scanning period of 1cm. This hologram is a Gabor-type hologram and the obtained hologram is shown in

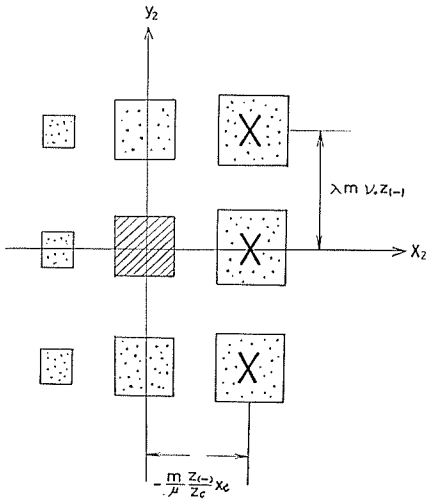

Fig. 21. Schematic configuration of the zero and first-order true images on the image plane reconstructed from a grating-like acoustical hologram by the two-beam interference method.

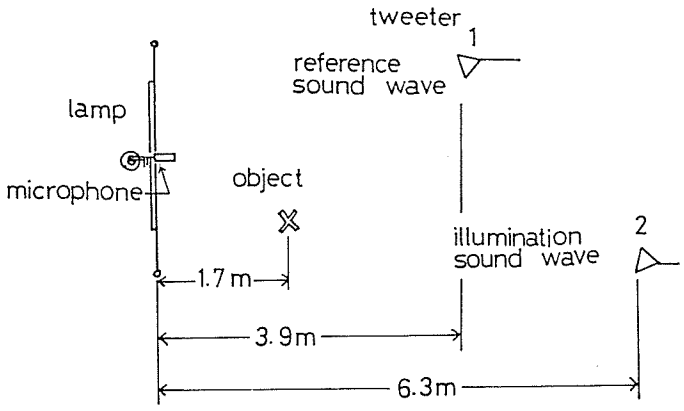

Fig. 22. Experimental arrangement for constructing acoustical holograms by the two-beam interference method.

Fig. 23-a. We construct holograms by intensifying the reference wave and we obtain the holograms of Fig. 23-b. In Fig. 23-b and c we see that the interference stripes constructed by the illumination wave and the reference wave appear.

The optical reconstruction of images is done in the optical system of Fig. 9. The reconstructed conjugate images from the hologram of Fig. 23-a and c are shown in Fig. 24-a and b. We observe that six kinds of images and their higher-order images are reconstructed from the hologram of Fig. 23-b where the intensity of the object and the reference wave is comparable. These six kinds of images are reconstructed as shown in Fig. 25 where each number shows the images; ① shifted inverse-contrast conjugate image, ② unshifted normal-contrast conjugate

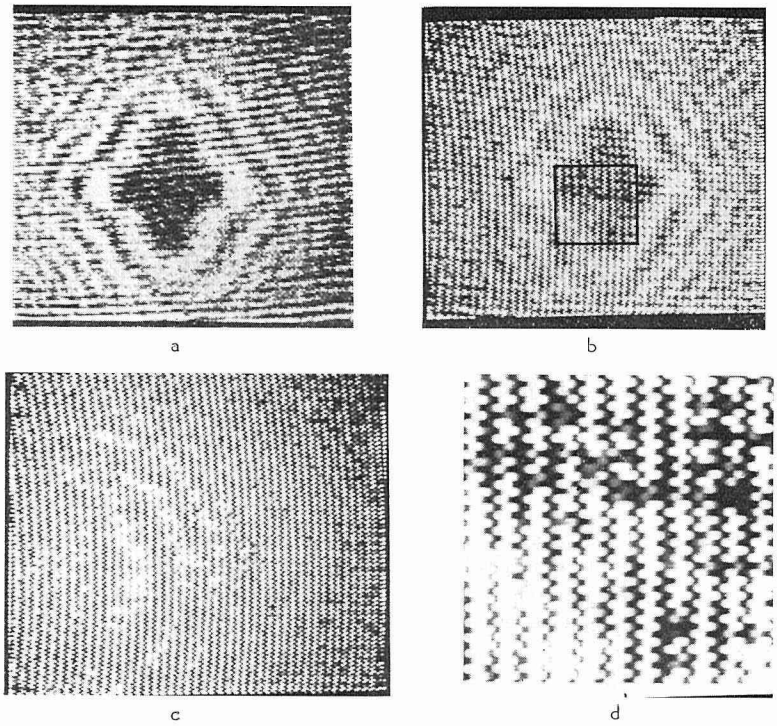

Fig. 23. Acoustical holograms constructed by the two-benm inerference method. In the holograms of a, the referenece wave is cut off, while the reference waves (the intensity of the reference wave in c is stronger than that in b) are appled in the holograms of b and c.

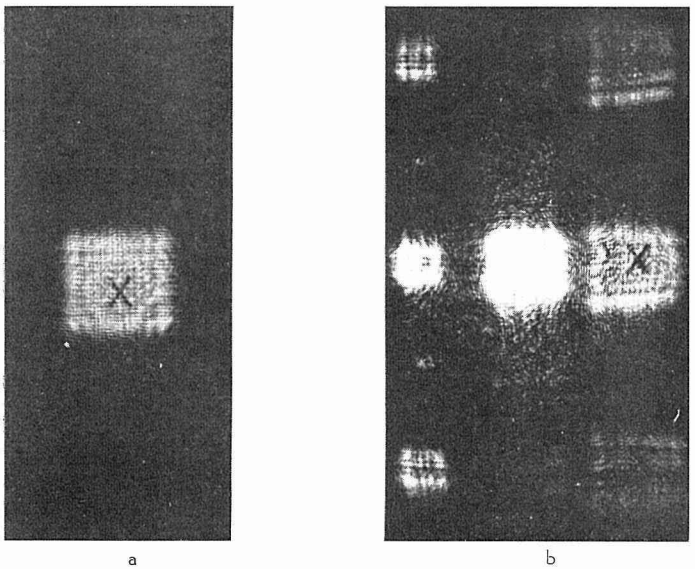

Fig. 24. Reconstructed conjugate images from the hologram of Fig. 23-a and c, where a and b corressond to Fig, 23-a and c, respectively.

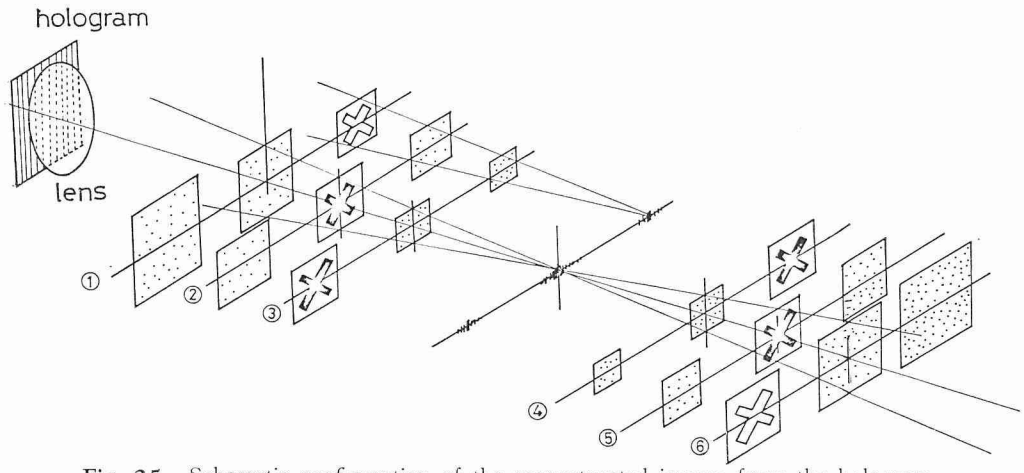

Fig. 25. Schematic configuration of the reconstructed images from the hologram of Fig. 23-b. ① shifted inverse-contrast conjugate image, ② unshifted normal-contrast conjugate image, ③ shifted normal-contrast conjugate image, ④ shifted normal-contrast true image, ⑤ unshifted normal-contrast true image, ⑥ shifted inverse-contrast true image.

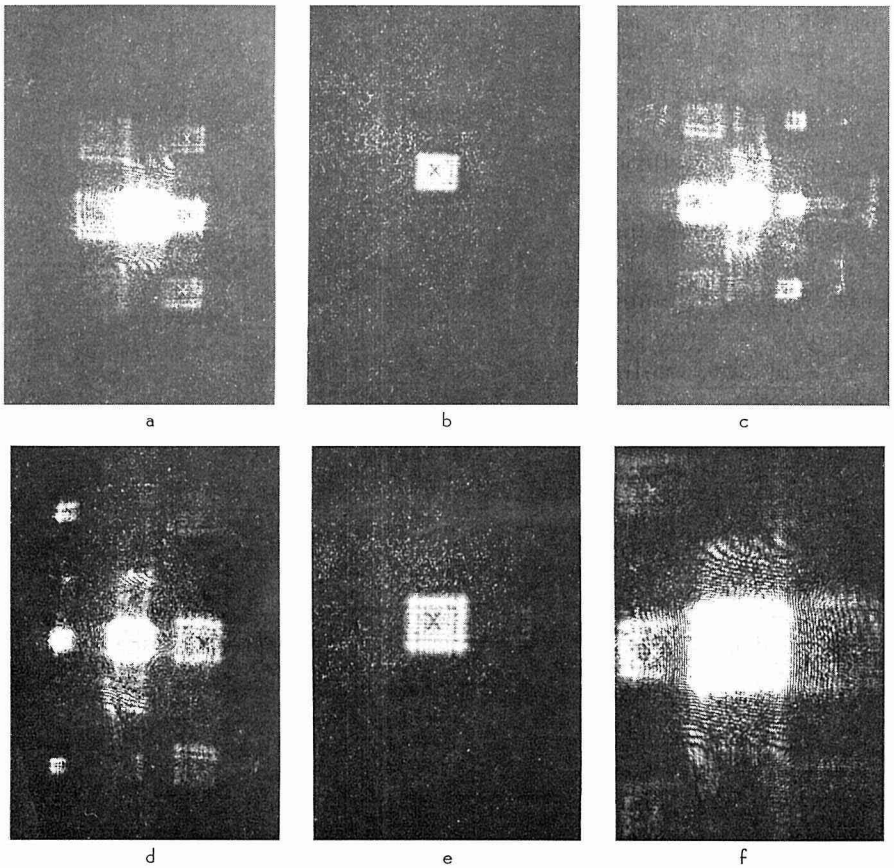

Fig. 26. Reconstructed images from the hologram of Fig. 23-b, where a. b, c, d, e, and f correspond to ①, ②, ③, ④, ⑤ and ⑥ of Fig. 25.

image, ③ shifted normal-contrast conjugate image, ④ shifted normal-contrast true image, ⑤ unshifted normal-contrast true image, and ⑥ shifted inverse-contrast true image. These image are shown in Fig. 26-a～f. The reason why the inverse-contrast images ① and ⑥ appear, can not be well explained, but it may be explained from a point of non-linear effect in holography.[28),29)]

In Fig. 26 the higher-order images appear and these higher-order images are reconstructed by the light diffracted by every other scanning lines because the time delay of the lamp causes the zigzag interference stripes as shown in Fig. 23-d.

2.5 Higher-order images reconstructed from acoustical holograms by an electronic reference method

In the preceding section we used reference sound-wave propagating through free space to construct the hologram. In acoustical holography we can simulate the reference wave electronically.[3),4),7),8),12),14)] In this section we discuss the reconstructed images from a grating-like acoustical hologram constructed with an electronic reference.

The acoustical holograms are constructed in the experimental arrangement shown in Fig. 27. The object is a letter cut on a screen made of a sheet paste-

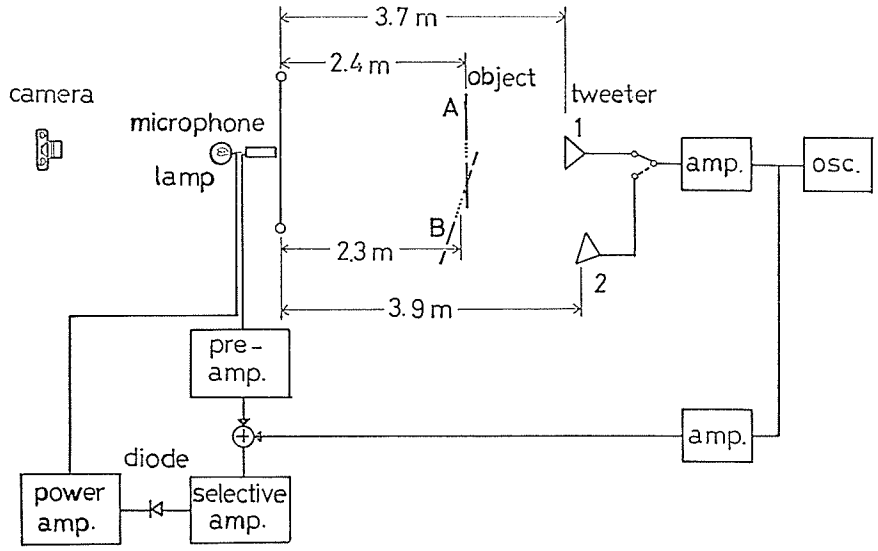

Fig. 27. Experimental arrangement for constructing acoustical holograms by the electronic reference method.

board as shown in Fig. 28. First, the letter S (the size is the same as the letter S shown in Fig. 7) of Fig. 28 is placed as A in Fig. 27. Acoustical holograms are constructed changing the frequency of the sound-waves where the reference plane waves are simulated electronically. The obtained holograms are shown in Fig. 29-a～c.

The optical reconstruction of images is done in the optical system of Fig. 9

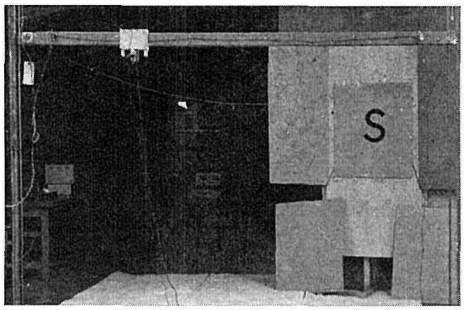

Fig. 28. Object (the letter *S*) and experimental equipment.

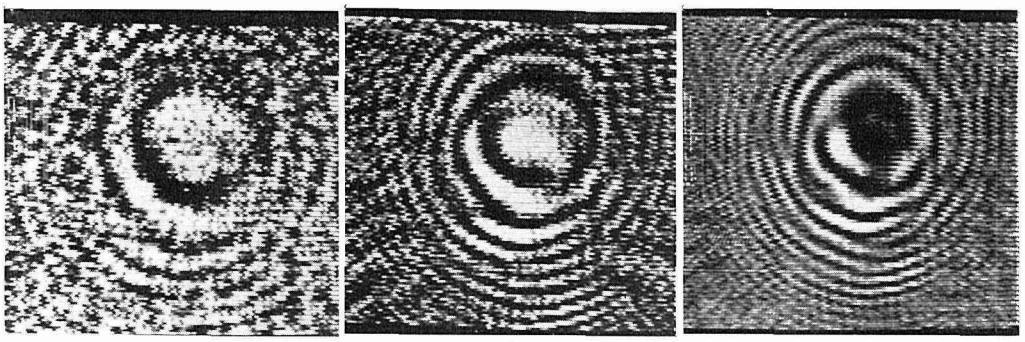

a b c

Fig. 29. Acoustical holograms constructed by simulating the reference waves electronically, where a, b, and c are constructed with sound-waves of 10 kHz, 15 kHz, and 20 kHz, respectively.

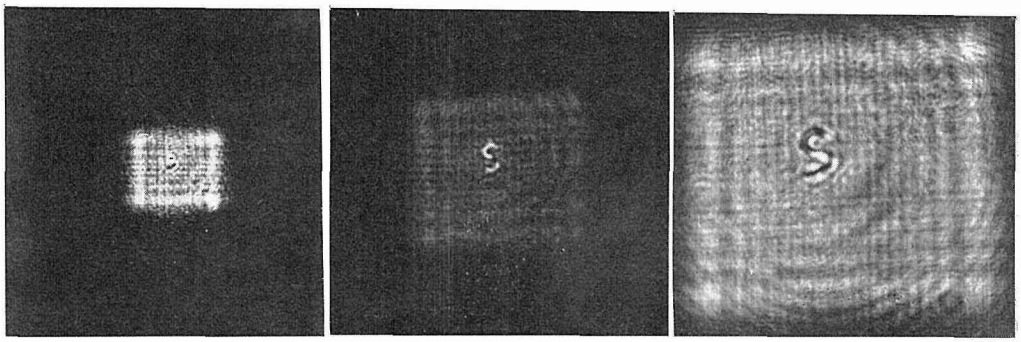

a b c

Fig. 30. Reconstructed true images from the holograms of Fig. 29, where a, b, and c correspond to Fig. 29-a, b, and c.

and the reconstructed true images are shown in Fig. 30-a～c where the images become unclear as the frequency of the sound-waves decreases, that is, the wavelength increases. The reason why the magnitude of reconstructed images increases as the wavelength the of sound-wave decreases can be explained from Eq. (12). We substitute $1/z_i=0$ and $x_i/z_i=0$ in Eqs. (11) and (12), because the simulated background illumination is a plane wave whose wavefront is parallel to the hologram plane and we can obtain the coordinates of the zero-order images as follows,

$$x_{2(\mp)} = \mp \frac{mFx_0}{\frac{\Lambda}{\lambda} z_0 \mp m^2 F} \tag{24}$$

where the negative and positive signs correspond to the true and conjugate images, respectively. In Eq. (24) the magnitude of the true image $x_{2(-)}$ increases as the wavelength Λ of the sound-wave decreases. The inverse-contrast image is reconstructed in Fig. 30-c. The reason why this inverse-contrast image appears is not well explained but it seems that the adjustment of electronic circuits causes this effect.

Next we construct an acoustical hologram where the letter S is placed as B in Fig. 27. In this experimental arrangement the object sound-wave beam inclines to the simulated reference plane-wave beam so that we can separate the image from background light in the optical reconstruction process. A grating-like acoustical hologram constructed in this arrangement by the sound-wave of 18 kHz is shown in Fig. 31 where the scanning period is chosen as 2 cm. The reconstructed

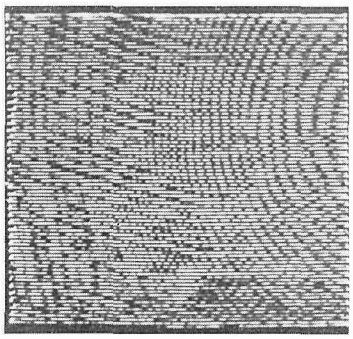

Fig. 31. Acoustical holograms constructed by simulating the reference wave electronically. The object is placed in a manner similar to B in Fig. 27.

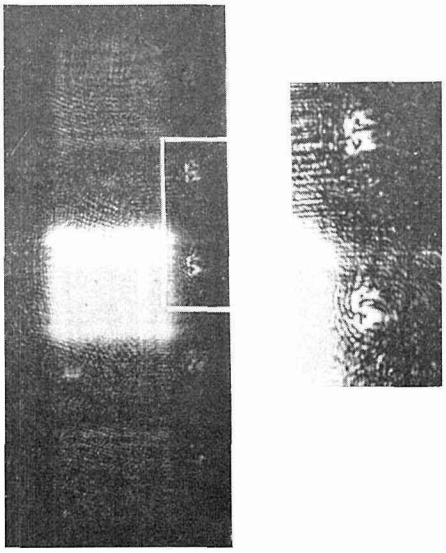

Fig. 32. Reconstructed conjugate images from the hologram of Fig. 31. The backgrounds are diffracted by each scanning line, while the images are diffracted by every other scanning lines.

conjugate images from the hologram of Fig. 31 is shown in Fig. 32 where the higher-order images are reconstructed. Figure 31 shows that the background is diffracted by each scanning line while the images are diffracted by every other scanning lines because of the time delay characteristics of the lamp as mentioned in section **2. 4**.

3. Space Division Multiplexing Acoustical Holography

3.1 Theory

The higher-order images reconstructed from a grating-like acoustical hologram are available for some applications, one of which is multiple information storage in a hologram. This holographic technique may be called a space division multiplexing holography[16] because this technique is similar to that of time division multiplex in a communication system. We explain the principle of this technique briefly.

We assume that there are N objects as shown in Fig. 33. We represent an illumination acoustical wave by b and the diffracted waves from the objects by

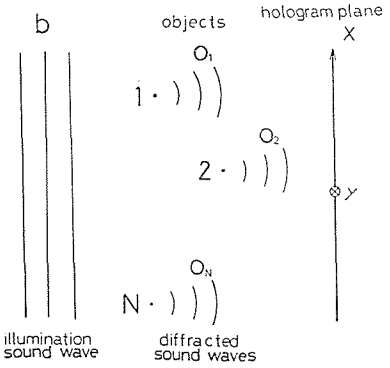

Fig. 33. Construction of an acoustical hologram of numerous objects, where the background sound-wave is expressed by b and the diffracted object waves are expressed by o_r $(r=1,2\cdots N)$.

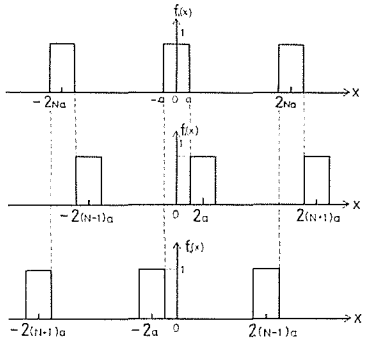

Fig. 34. Method of scanning for constructing a space division multiplexing acoustical hologram.

o_r $(r=1,2\cdots N)$. In the proposed technique we record the hologram of object 1 by the scanning of $f_1(x)$ shown in Fig. 34 with a microphone when there is only object 1 in Fig. 33. Next we record the hologram of object 2 by the scanning of $f_2(x)$ of Fig. 34 which does not overlap with the scanning of $f_1(x)$, when there is only object 2. We continue this procedure untill we record the hologram of N-th object and construct a single hologram which stores the information of different objects of N pieces. The obtained hologram H in this procedure is represented by,

$$\begin{aligned} H &= f_1(x)[|b|^2+|o_1|^2+b^*o_1+bo_1^*] \\ &\quad + f_2(x)[|b|^2+|o_2|^2+b^*o_2+bo_2^N] \\ &\quad \vdots \\ &\quad + f_N(x)[|b|^2+|o_N|^2+b^*o_N+bo_N^*] \\ &= |b|^2+\sum_{r=1}^{N} f_r(x)|o_r|^2+\sum_{r=1}^{N} f_r(x)(b^*o_r+bo_r^*) \end{aligned} \tag{25}$$

where the function $f_r(x)$ of the scanning lines is represented by,

$$f_r(x)=\frac{1}{N}\left[1+2\sum_{m=1}^{\infty}\frac{\sin(2\pi na\nu_0)}{2\pi na\nu_0}\cos 2\pi n\nu_0\{x-2(r-1)a\}\right]. \tag{26}$$

In this technique the hologram space is divided into N sections by the scanning of a microphone to record information of each object in each divided hologram space. This technique has an advantage compared to the multi-exposure recording of holograms. If the holograms of N objects are recorded by multi-exposure recording of N times, the obtained hologram is represented by,

$$\begin{aligned}H&=(b+o_1)(b+o_1)^*+(b+o_2)(b+o_2)^*+\cdots+(b+o_N)(b+o_N)^*\\&=N|b|^2+\sum_{r=1}^{N}|o_r|^2+\cdots+\sum_{r=1}^{N}(b^*o_r+bo_r^*)\end{aligned} \tag{27}$$

where the recording system (film) is assumed to be linear for the intensity of acoustical fields. In the hologram of Fig. (27) the bias term becomes N times the bias term $|b|^2$ of the hologram of a single object and this indicates that, as the number N increases, the images are disturbed by a strong bias light, resulting in invisible images. On the other hand the higher-order images reconstructed from the hologram of Eq. (25) are separated from the bias light and we obtain high-contrast images even if the intensity of image term is not stronger than that of the hologram of Eq. (27).

Further we can divid the hologram space by the scanning direction of a microphone. We assume that there are N objects by x_{0r} $(r=1,2\cdots N)$ as shown in Fig. 35. First, we record the hologram of object 1 by scanning perpendicular to

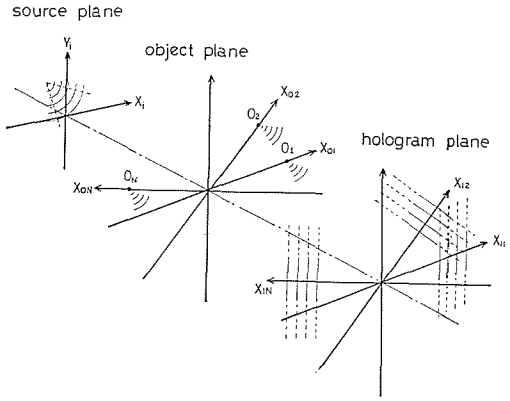

Fig. 35. Construction of an acoustical hologram, where the hologram is constructed by changing the scanning direction of a microphone.

the axis x_{11} with the scanning frequency ν_{01} as shown in Fig. 35, when there is only object 1. Next we record the hologram of the object 2 by the scanning perpendicular to the axis x_{12} with the scanning frequency ν_{02} when there is only object 2. We continue this procedure until we record the hologram of N-th object and construct a single hologram. We reconstruct this hologram in the optical system of Fig. 9. Then the coordinates of images are obtained from Eqs.

(10) and (11),

$$\begin{bmatrix} x_{21} \\ x_{22} \\ \vdots \\ x_{2r} \\ \vdots \\ x_{2N} \end{bmatrix} = \frac{1}{\left[\frac{1}{F} \mp \frac{m^2}{\mu}\left(\frac{1}{z_0} - \frac{1}{z_i}\right)\right]} \begin{bmatrix} \mp \frac{m}{\mu}\left(\frac{x_{01}}{z_0} - \frac{x_i}{z_i}\right)(\pm)\lambda mn\nu_{01} \\ \mp \frac{m}{\mu}\left(\frac{x_{02}}{z_0} - \frac{x_i}{z_i}\right)(\pm)\lambda mn\nu_{02} \\ \vdots \\ \mp \frac{m}{\mu}\left(\frac{x_{0r}}{z_0} - \frac{x_i}{z_i}\right)(\pm)\lambda mn\nu_{0r} \\ \vdots \\ \pm \frac{m}{\mu}\left(\frac{x_{0N}}{z_0} - \frac{x_i}{z_i}\right)(\pm)\lambda mn\nu_{0N} \end{bmatrix}. \quad (28)$$

Equation (28) shows that the higher-order images are reconstructed along each direction perpendicular to each scanning direction. The reconstructed higher-order images have an advantage in that the higher-order images are reconstructed separately from each other even if the objects are placed closely and the reconstructed zero-order images overlap.

3.2 Experiment

A space division multiplexing acoustical hologram is constructed in the experimental arrangement of Fig. 36 where two tweeters and two objects (the letter

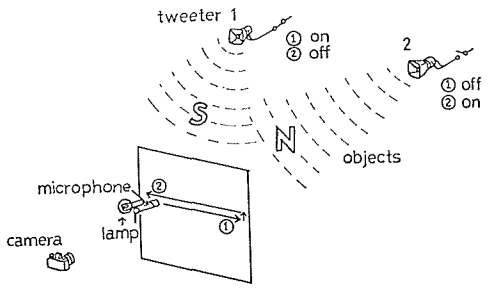

Fig. 36. Experimental arrangement for constructing a space division multiplexing acoustical hologram. At the time of scanning ① of a microphone, tweeter 1 radiates a sound-wave and information of the letter S is recorded, while tweeter 2 is cut off. Alternately, tweeter 2 radiates a sound-wave while tweeter 1 is cut off, and information of the letter N is recorded during scanning ②.

S and N) are prepared. Figure 37 is the photograph of these objects and the experimental equipment. The distances from the microphone to the objects, tweeter 1 and tweeter 2 are 1.7 m, 3.9 m and 6.3 m, respectively. An acoustical hologram is constructed in the process, where tweeter 1 radiates a sound wave to illuminate the letter S at the time of forward scanning of the microphone (denoted ① in Fig. 36) and a camera records the information of letter S when tweeter 2 is cut off, and at the time of backward scanning of the microphone (denoted ② in Fig. 36), tweeter 2 radiates a sound wave to illuminate the letter

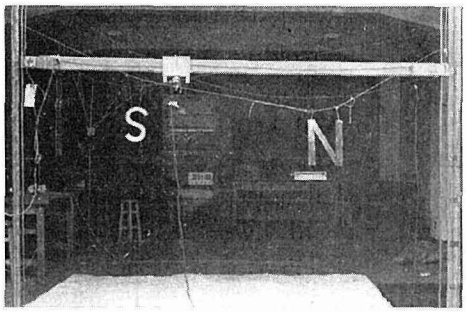

Fig. 37. Objects (the letters S and N) and experimental equipment.

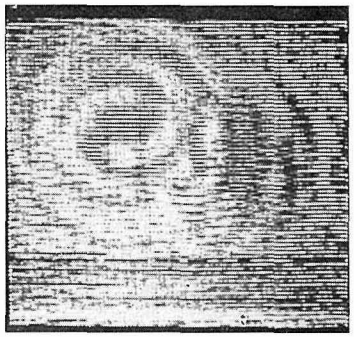

Fig. 38. Space division multiplexing acoustical hologram.

N and the camera records the information of letter N when tweeter 1 is cut off. A sound wave hologram constructed in this manner is shown in Fig. 38 where the scanning is done with scanning period of 1 cm, ie. the scanning period 2Na of Fig. 34 for each object is 2 cm. The frequency of the sound wave is chosen as 15 kHz.

The reconstructed conjugate images from the hologram of Fig. 38 are shown in Fig. 39-a and b. In Fig. 39 only the first-order images appear separately from the bias light and the zero-order images disappear because the zero-order images are disturbed by a strong background while the first-order images are not disturbed as shown in Eq. (25). These images are reconstructed at different image planes because the curvatures of sound-waves from tweeter 1 and 2 are different at the object plane. In Fig. 39 the inverse-contrast images appear because the acoustical

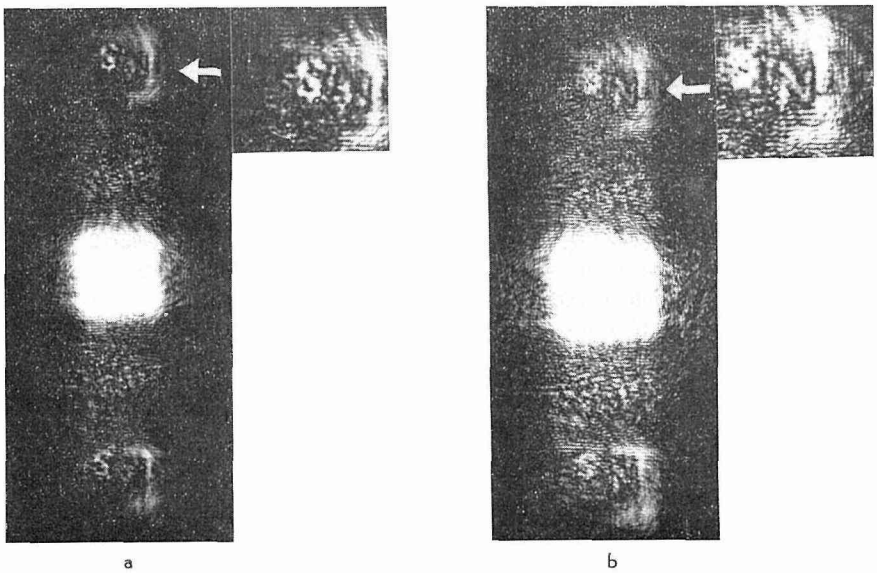

a b

Fig. 39. Reconstructed conjugate images of letters S(a) and N(b) from the hologram of Fig. 38.

hologram of Fig. 38 is similar to the [III]-type grating-like hologram in Table 1.

To compare the images of Fig. 39 with the image reconstructed from the hologram of Eq. (27), an acoustical hologram is constructed by double exposure in the arrangement of Fig. 36. In this case tweeter 1 radiates a sound-wave to illuminate the letter S and a camera records the hologram of S on a film while tweeter 2 is cut off and, in turn, tweeter 2 radiates a sound-wave to illuminate the letter N and the camera records the hologram of N on the preceding hologram of S while tweeter 1 is cut off. The obtained hologram is shown in Fig. 40 where the scanning period is chosen as 1 cm for each object. The reconstructed

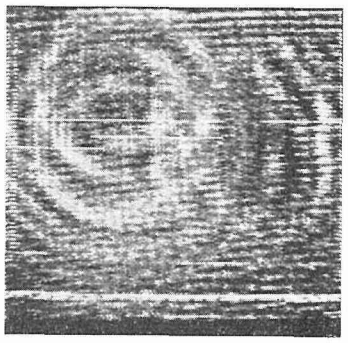

Fig. 40. Acoustical hologram constructed by double exposure.

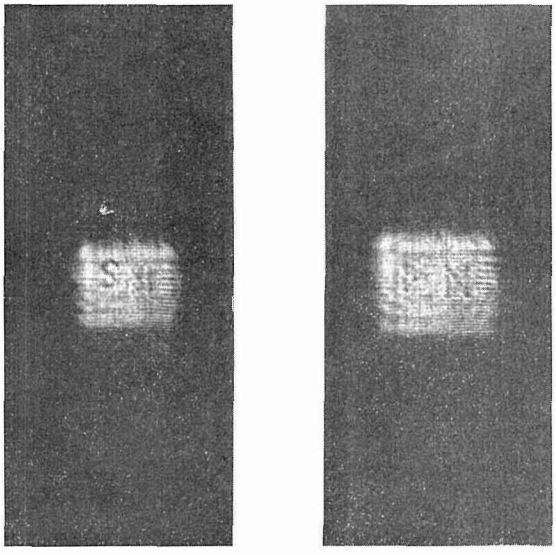

a b

Fig. 41. Reconstructed conjugate images of letters S (a) and N (b) from the hologram of Fig. 40.

conjugate images from the hologram of Fig. 40 are shown in Fig. 41-a and b. Comparing the reconstructed images of Fig. 39 with Fig. 41, we see that the images of Fig. 39 are higher-contrast images than those of Fig. 41.

In this experiment the same scanning periods, that is, the same sampling frequencies are chosen for the objects S and N, but we can choose different sampling frequencies to record varied information. For example if different sampling frequencies are chosen for different wavelengths of illuminating sound-waves to construct a hologram, the higher-order images are reconstructed separately from each other according to the wavelength so that the wavelength characteristics of an object can be reconstructed from a single acoustical hologram.

Further an acoustical hologram is constructed, where the information of different objects is recorded by changing the scanning direction of the microphone as shown in Fig. 35. First a sound-wave is applied to the letter S and a hologram of the letter S is recorded on a film by horizontal scanning of the microphone.

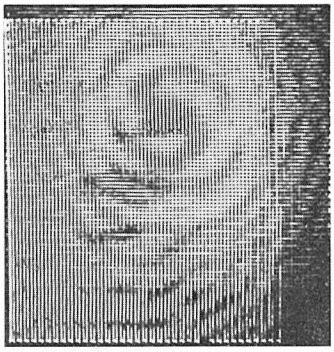

Fig. 42. Acoustical hologram in which the letter S is recorded by horizontal scanning, while the hologram of the letter N is recorded by vertical scanning produced by rotating the camera 90°.

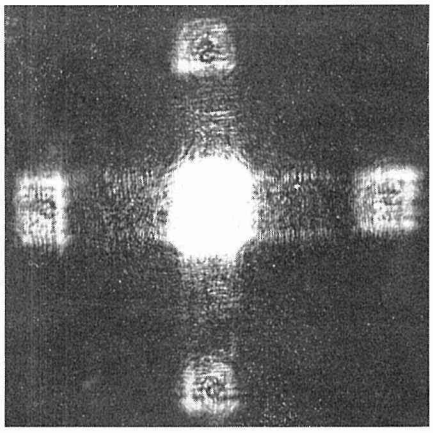

Fig. 43. Reconstructed conjugate images from the hologram of Fig. 42.

Next the camera is rotated 90° and a sound-wave is applied to the letter N and the hologram of the letter N is recorded on the preceding hologram of the letter S. In this procedure, a rotation of the camera is equivalent to changing the scanning direction of the microphone. The obtained hologram is shown in Fig. 42 where the scanning periods are chosen as 2 cm for each object. The reconstructed conjugate images from the hologram of Fig. 42 are shown in Fig. 43 where the first-order images of S and N are reconstructed separately according to the scanning directions of the microphone.

In this experiment the recorded objects in a hologram are two simple objects, but this technique is applicable for the storage of varied information of numerous objects. If we use two-dimensional arrays of receivers and introduce the electronic scanning instead of the mechanical scanning, we record the hologram of moving object in a single hologram by changing the scanning direction for different moments and we observe the image of different moments from the higher-order images reconstructed separately corresponding to the scanning direction.

4. Multi-Color Acoustical Holography

4.1 Theory

A grating-like acoustical hologram reconstructs higher-order images when it is illuminated by a monochromatic light such as laser light. If the grating-like acoustical hologram is illuminated by a polychromatic light, each spectrum of the light reconstructs the higher-order images and generally these images overlap and the reconstructed images disappear. However, if we can separate these images reconstructed by each spectrum of polychomatic light under certain conditions, we can reproduce multi-color images[30] from the grating-like acoustical holograms. In this section we discuss the conditions for reconstructing a single-color image by polychromatic light and we propose an optical system to obtain a multi-color image using grating-like acoustical holograms.

First we discuss the relation between the spatial frequencies of the hologram and their spectrum on the Fourier-transform plane by the matrix method. A hologram contains many spectra of spatial frequencies. Here we select one spectrum which is translated to a ray position on the spectrum plane. In other words we assume a patch of a hologram which consists of one spectrum of spatial frequency $m\nu$, that is, we assume a hologram to be a part of a diffraction grating of the spatial frequency $m\nu$ as shown in Fig. 44. This grating modulates the

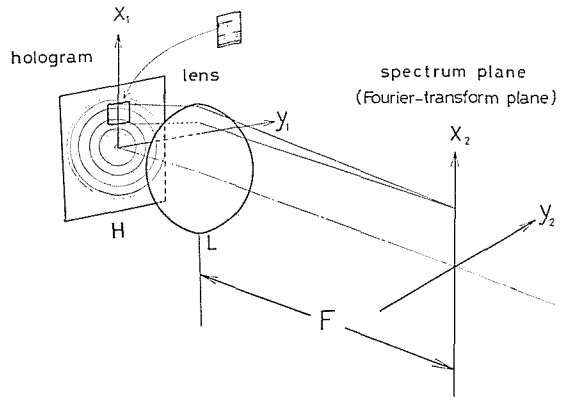

Fig. 44. Transformation of the spatial frequency of the hologram to the ray position on the Fourier-transform plane.

grating of the scanning lines of the spatial frequency $m\nu_0$ if the scanning lines appear on the hologram and the spatial frequency $m\nu_0$ is sufficiently larger than that of the hologram. We obtain the spectra of the grating-like hologram, that is, the coordinates of the rays diffracted by the gratings of the spatial frequencies $m\nu$ and $m\nu_0$ at the focal plane of lens L in Fig. 44, from the matrices of Eqs. (1), (2) and (6),

$$\begin{bmatrix} x_2 \\ x_2' \end{bmatrix} = \begin{bmatrix} 1 & F \\ 0 & 1 \end{bmatrix} \begin{bmatrix} 1 & 0 \\ -\frac{1}{F} & 1 \end{bmatrix} \left\{ \begin{bmatrix} 1 & 0 \\ 0 & 1 \end{bmatrix} \begin{bmatrix} x_1 \\ 0 \end{bmatrix} + \begin{bmatrix} 0 \\ \pm \lambda m\nu \end{bmatrix} + \begin{bmatrix} 0 \\ \pm \lambda mn\nu_0 \end{bmatrix} \right\}$$
$$= \begin{bmatrix} 0 & F \\ -\frac{1}{F} & 1 \end{bmatrix} \begin{bmatrix} x_1 \\ 0 \end{bmatrix} + \begin{bmatrix} \pm \lambda mF(n\nu_0 \pm \nu) \\ \pm \lambda m(n\nu_0 \pm \nu) \end{bmatrix}. \tag{29}$$

When monochromatic light (wavelength λ_1) is applied to the grating-like hologram the spectrum distribution can be drawn schematically as shown in Fig. 45-a. Next we assume that the ideal polychromatic light of two discrete spectra (the wavelengths λ_1 and λ_2) is applied to the grating-like hologram and the spectrum distribution is drawn as shown in Fig. 45-b. We discuss the conditions for reconstructing a single-color image from the relations of wavelength separation $\Delta\lambda = (\lambda_2 - \lambda_1)$ and the bandwidth $\Delta\nu$ defined to include sufficient spectra in reconstructing images. If the spectra of the higher-order images can be separated according to the spectra $\lambda_1\nu_0$ and $\lambda_2\nu_0$ of polychromatic light, we can reconstruct the single-color

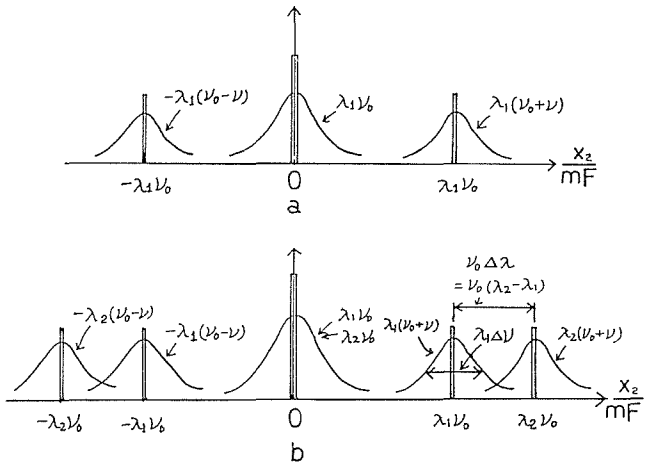

Fig. 45. Spectrum distribution of a grating-like hologram. In a, the hologram is illuminated by monochromatic light of a wavelength λ_1, while in b, the hologram is illuminated by polychromatic light of two wavelengths λ_1 and λ_2. ν_0 is a fundamental spatial frequency of the grating and ν is the spatial frequencies of the hologram.

image by specific selection of only the spectra belonging to the wavelength λ_1 (or λ_2) at the spectrum plane. In Fig. 45-b we obtain this condition,

$$\frac{\Delta\lambda}{\lambda} \geqq \frac{\Delta\nu}{\nu_0} \tag{30}$$

This condition indicates that we must choose a polychromatic light of discrete or nearly discrete spectra and that the wavelength separation $\Delta\lambda$ of the nearest neighboring spectra must be large and moreover the sampling frequency should be sufficiently high as compared with the bandwidth $\Delta\nu$ of the hologram.

Now we discuss the optical system to construct a multi-color acoustical image when single-color images are reconstructed from grating-like holograms by polychromatic light of discrete spectra. We construct a grating-like acoustical hologram and arrange its reduced hologram for optical reconstruction as shown in Fig. 46-a. In Fig. 46-a the scanning lines run parallel to the y_{01} axis and the center of the hologram $x_{01}=b$. In the arrangement of Fig. 46-a the hologram is represented by the following matrix equation,

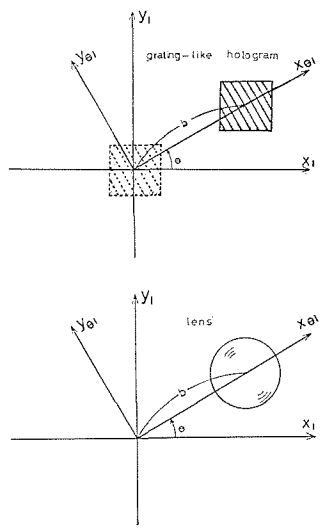

Fig. 46. Arrangement of a grating-like acoustical hologram and a convex lens for optical reconstruction of images.

$$\begin{bmatrix} x_{\theta 2} \\ x'_{\theta 2} \\ y_{\theta 2} \\ y'_{\theta 2} \end{bmatrix} = \begin{bmatrix} 1 & 0 & 0 & 0 \\ \pm\dfrac{m^2}{\mu}\left(\dfrac{1}{z_0}-\dfrac{1}{z_i}\right) & 1 & 0 & 0 \\ 0 & 0 & 1 & 0 \\ 0 & 0 & \pm\dfrac{m^2}{\mu}\left(\dfrac{1}{z_0}-\dfrac{1}{z_i}\right) & 1 \end{bmatrix} \begin{bmatrix} x_{\theta 1} \\ x'_{\theta 1} \\ y_{\theta 1} \\ y'_{\theta 1} \end{bmatrix}$$

$$+ \begin{bmatrix} 0 \\ \mp\dfrac{m}{\mu}\left(\dfrac{x_0\cos\theta + y_0\sin\theta + b}{z_0} - \dfrac{x_i\cos\theta + y_i\sin\theta + b}{z_0}\right)(\pm)\lambda m n \nu_0 \\ 0 \\ \mp\dfrac{m}{\mu}\left(\dfrac{y_0\cos\theta - x_0\sin\theta}{z_0} - \dfrac{y_i\cos\theta - x_i\sin\theta}{z_i}\right) \end{bmatrix}. \tag{31}$$

The matrix representation of a convex lens whose center is $x_{\theta 1}=b$ and $y_{\theta 1}=0$ as shown in Fig. 46-b, is as follows,

$$\begin{bmatrix} x_{\theta 2} \\ x'_{\theta 2} \\ y_{\theta 2} \\ y'_{\theta 2} \end{bmatrix} = \begin{bmatrix} 1 & 0 & 0 & 0 \\ -\dfrac{1}{F} & 1 & 0 & 0 \\ 0 & 0 & 1 & 0 \\ 0 & 0 & -\dfrac{1}{F} & 1 \end{bmatrix} \begin{bmatrix} x_{\theta 1} \\ x'_{\theta 1} \\ y_{\theta 1} \\ y'_{\theta 1} \end{bmatrix} + \begin{bmatrix} 0 \\ \dfrac{b}{F} \\ 0 \\ 0 \end{bmatrix}. \tag{32}$$

We assume that -1 order image is reconstructed by polychromatic light in Fig. 47 where the spectra belonging to a certain wavelength of polychromatic light is selected at the focal plane of the lens L. The coordinates of the image are obtained from the matrices of the free space and Eqs. (31) and (32) by,

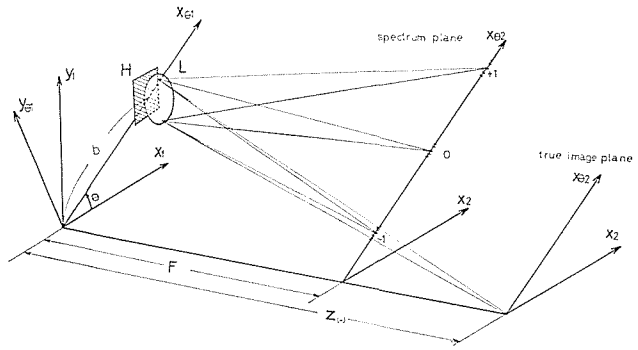

Fig. 47. Optical arrangement for constructing a single-color image from a grating-like hologram. Spectra of narrow bandwidth are selected from the -1 order spectra at the focal plane of lens L.

$$\begin{bmatrix} x_{\theta 2} \\ y_{\theta 2} \end{bmatrix} = \begin{bmatrix} \cos\theta & \sin\theta \\ -\sin\theta & \cos\theta \end{bmatrix} \begin{bmatrix} -z_{(-)} \dfrac{m}{\mu}\left(\dfrac{x_0}{z_0} - \dfrac{x_i}{z_i}\right) \\ -z_{(-)} \dfrac{m}{\mu}\left(\dfrac{y_0}{z_0} - \dfrac{y_i}{z_i}\right) \end{bmatrix} + \begin{bmatrix} bz_{(-)}\left\{-\dfrac{m^2}{\mu}\left(\dfrac{1}{z_0} - \dfrac{1}{z_i}\right) + \dfrac{1}{F}\right\} - \lambda m \nu_0 z_{(-)} \\ 0 \end{bmatrix} \tag{33}$$

where $z_{(-)}$ is the distance from the hologram to the image plane and may be obtained as follows,

$$\frac{1}{z_{(-)}} = \frac{1}{F} - \frac{\lambda m^2}{A}\left(\frac{1}{z_0} - \frac{1}{z_i}\right). \tag{34}$$

In Eq. (33), we choose b to satisfy the following relation,

$$b = \frac{\lambda m \nu_0}{\dfrac{1}{F} - \dfrac{m^2}{\mu}\left(\dfrac{1}{z_0} - \dfrac{1}{z_i}\right)} \tag{35}$$

Using Eq. (35), Eq. (31) is rewritten,

$$\begin{bmatrix} x_{\theta 2} \\ y_{\theta 2} \end{bmatrix} = \begin{bmatrix} \cos\theta & \sin\theta \\ -\sin\theta & \cos\theta \end{bmatrix} \begin{bmatrix} x_{\theta 2}|_{\theta=0} \\ y_{\theta 2}|_{\theta=0} \end{bmatrix}. \tag{36}$$

Equation (36) indicates that the postion of the reconstructed image is independent of the angle θ in Fig. 47. From Eq. (33) we obtain the following image coordinates,

$$\begin{aligned} x_{\theta 2}|_{\theta=0} &= -z_{(-)} \cdot \frac{\lambda m}{A}\left(\frac{x_0}{z_0} - \frac{x_i}{z_i}\right) \\ y_{\theta 2}|_{\theta=0} &= -z_{(-)} \cdot \frac{\lambda m}{A}\left(\frac{y_0}{z_0} - \frac{y_i}{z_i}\right). \end{aligned} \tag{37}$$

We obtain a multi-color image by overlapping the single-color images, but the magnitude and the position of the image are not constant for different wavelengths λ of polychromatic light as shown in Eqs. (34) and (37). Therefore we must keep the magnitude $x_{\theta 2}$, $y_{\theta 2}$ and the position $z_{(-)}$ of the single-color images constant for each spectrum to reconstruct a multi-color image by polychromatic light. From Eqs. (34) and (37) we obtain the condition for reconstructing a multi-color image which is as follows,

$$\frac{\lambda}{A} = \text{constant} \tag{38}$$

This condition indicates that we must distribute the spectra of polychromatic light to the reconstracted images proportionally to the spectra of the sound-waves. If we keep b constant for every spectra in Eq. (35), we obtain the following condition,

$$\lambda\nu_0 = \text{constant} \tag{39}$$

Using this condition we can select the spectra of polychromatic light by the concentric circle opening of radius $(b-\lambda m\nu_0 F)$ for reconstructing a multi-color image as shown in Fig. 48. If there is an ideal polychromatic light with the discrete

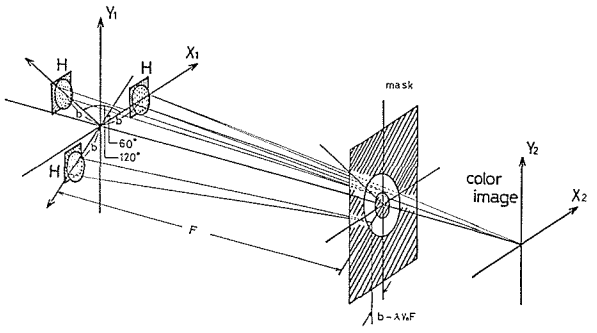

Fig. 48. Optical arrangement for constructing a multi-color image using grating-like holograms.

spectra of three primary colors, we could reconstruct a multi-color image in the arrangement of Fig. 48 where three grating-like acoustical holograms constructed by sound-waves of three different frequencies are used.

4.2 Preliminary experiment

For a preliminary experiment to construct a multi-color acoustical image, an experiment to reconstruct a single-color image by polychromatic light from a grating-like acoustical hologram is conducted. The acoustical hologram of Fig. 8-c is used in this experiment. The reconstructed images from the hologram of Fig. 8-c are used in this experiment. The reconstructed images from the hologram of Fig. 8-c using a laser light in the optical system of Fig. 9 are shown in Fig. 11-c.

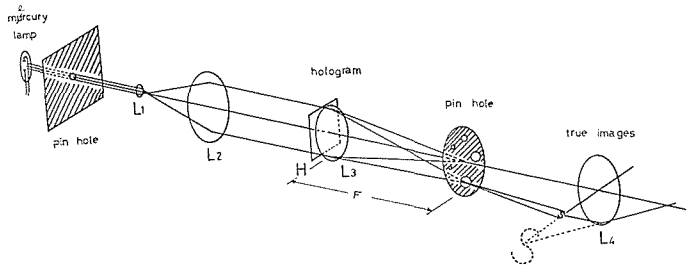

Fig. 49. Optical system for reconstructing single-color images from a grating-like hologram. A mercury lamp is used for the polychromatic light source.

Here the reconstruction of single-color images is done in the optical system of Fig. 49 where a mercury lamp is used as a polychromatic light source. The spectra of polychromatic light diffracted by the scanning lines of the hologram appear in the focal plane of lens L_3 in Fig. 49. These spectra from the hologram

of Fig. 8-c are shown in Fig. 50-a while Fig. 50-b shows the spectra of the spatial frequencies of the hologram reconstructed by laser light at the focal plane of lens L_3 in Fig. 49. The light distribution by the spectra of Fig. 50-a at the image plane is shown in Fig. 51 where we can not observe any distinct image. Next we set a pin hole at the focal plane of lens L_3 and thus select narrow bandwidth spectra and observe the image reconstructed by these spectra. The obtained images are shown in Fig. 52-a and b. In Fig. 52 we can hardly recognize the images, but there appears something like the image of the letter S in the almost single-colored background. If a more suitable polychromatic light source of discrete spectra is chosen and the hologram-construction and image-reconstruction techniques are developed, finer single-color images can be obtained from the grating-like acoustical holograms, and a multicolor image can be obtained from the single-color images according to the procedure mentioned in the previous section.

5. Conclusion

Grating-like acoustical holograms are constructed by scanning with a microphone with coarse scanning periods. These acoustical holograms reconstruct higher-order images in the optical reconstruction process and these images have some properties, for example, contrast enhancement and contrast inversion. These properties come from the non-linearity of the hologram recording system and the property of the grating. These grating-like acoustical holograms are available for some applications, for example space division multiplexing acoustical holography and multi-color acoustical holography. The theoretical and experimental results suggest that the space division multiplexing holography is a technique useful for multiple information storage in a long wavelength hologram which is constructed by the scanning of a receiver or a detector. If a long wavelength hologram is constructed using two-dimensional arrays of receivers (or detectors) and electronic scanning, this technique can be extended to the recording of information of a moving object in a single long wavelength hologram. The application of grating-like acoustical holograms to multi-color acoustical holography is in a primitive stage now and there are many problems to be solved to develop this technique. However this technique has a potential usefulness for the application of the grating-like holograms.

Acknowledgment

The author wishes to thank Dr. M. Suzuki of the Hokkaido University for giving him the opportunity to conduct experiments related to the present work. He also wishes to thank Dr. T. Asakura for his discussion on holography and suggestions for writing the manuscript. The author is also indebted to I. Fukai, T. Sawai and other staff members and graduate students of the Electronics Engineering Department for their help in this work.

The present work is supported by a research fund given by the Fuji Photo Film Company to which the author is most grateful.

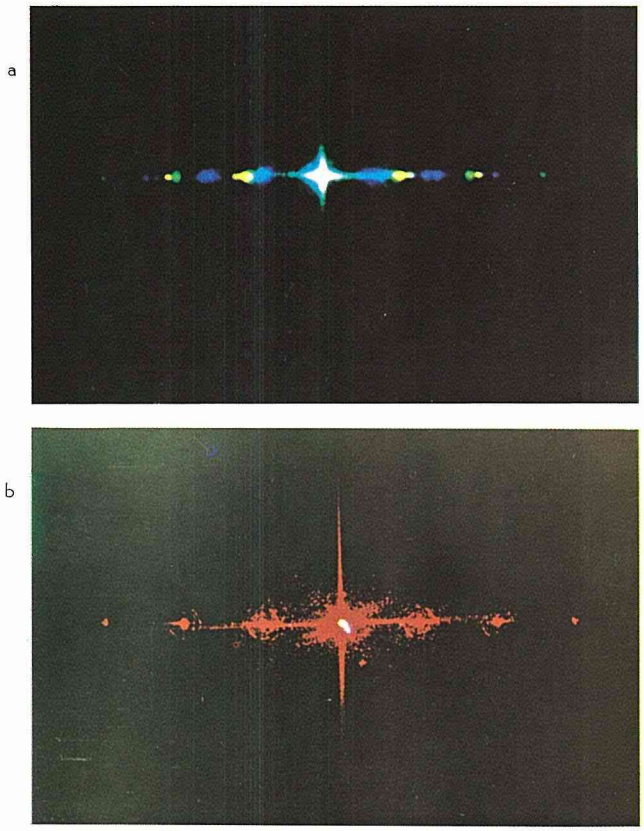

Fig. 50. Spectra of the grating-like acoustical hologram of Fig. 8-c. Spectra by polychromatic light of a mercury lamp are shown in a and spectra by monochromatic laser light are shown in b.

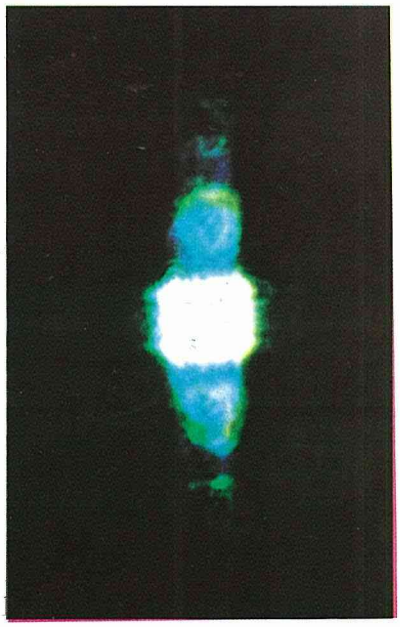

Fig. 51. Light distribution by the spectra of Fig. 50-a at the plane of the true image.

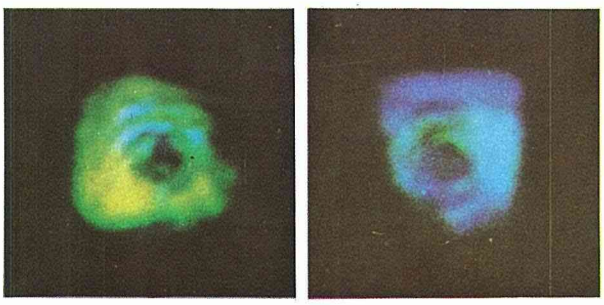

Fig. 52. Images in an almost single-colored background reconstructed from the hologram of Fig. 8-c in the optical system of Fig. 49.

References

1) R. K. Mueller and N. K. Sheridon: "Sound holograms and optical reconstruction", Appl. Phys. Letters, **9**, p. 328 (1966).
2) P. Greguss: "Techniques and information content of sonoholograms", J. Photo. Sci., **14**, p. 329 (1966).
3) K. Preston, Jr. and J. L. Kreuzer: "Ultrasonic imaging using a synthetic holographic technique", Appl. Phys. Letters, **10**, p. 150 (1967).
4) J. L. Kreuzer: "Ultrasonic three-dimensional imaging using holographic technique", Proceedings of the Symposium on Modern Optics, (Polytechnic Press), p. 91 (1967).
5) A. F. Metherell, H. M. A. El-Sum, J. J. Dreher and L. Larmore: "Optical reconstruction from sampled holograms with sound waves", Phys. Letters, **24-A**, p. 547 (1967).
6) A. F. Metherell, H. M. A. El-Sum, J. J. Dreher and L. Larmore: "Image reconstruction from sampled acoustic holograms", Appl. Phys. Letters, **10**, p. 277 (1967).
7) G. A. Massey: "Acoustic holography in air with an electronic reference", Proc. IEEE, **55**, p. 1115 (1967).
8) A. F. Metherell and H. M. A. El-Sum: "Simulated reference in a coarsely sampled acoustical hologram", Appl. Phys. Letters, **11**, p. 20 (1967).
9) Y. Aoki, N. Yoshida, N. Tsukamoto and M. Suzuki: "Sound wave hologram and optical reconstruction", Proc. IEEE, **55**, p. 1622 (1967).
10) Y. Aoki: "Three-dimensional information storage in an acoustic hologram", Appl. Opt., **7**, p. 1402 (1968).
11) Y. Aoki: "Acoustic Holograms and Optical Reconstruction", Acoustical Holography Vol. **1** (Prenum Press, New York, 1969) p. 223.
12) R. B. MacAnally: "Inclined reference acoustic holography", Appl. Phys. Letters, **11**, p. 266 (1967).
13) E. Maron, D. Fritzler and R. K. Mueller: "Ultrasonic holography by electronic scanning of a piezoelectric crystal", Appl. Phys. Letters, **12**, p. 26 (1968).
14) E. Maron, D. Fritzler and R. K. Mueller: "Electronic simulation of a variable inclination reference for acoustic holography via the ultrasonic camera", Appl. Phys. Letters, **12**, p. 394 (1968).
15) A. F. Metherell and S. Spinak: "Acoustical holography of nonexistent wavefronts detected at a single point in space", Appl. Phys. Letters, **13**, p. 22 (1968).
16) Y. Aoki: "Space division multiplexing holography", Proc. IEEE, **57**, p. 358 (1969).
17) R. P. Dooley: "X-band holography", Proc. IEEE, **53**, p. 1733 (1965).
18) W. E. Kock: "Hologarm television", Proc. IEEE, **54**, p. 331 (1966).
19) G. Tricoles and E. L. Rope: "Reconstruction of visible images from reduced-scale replicas of microwave holograms", J. Opt. Soc. Am., **57**, p. 97 (1967).
20) Y. Aoki: "Microwave holograms and optical reconstruction", Appl. Opt., **6**, p. 1943 (1967).
21) Y. Aoki: "Microwave holography by a two-beam interference method", Proc. IEEE, **56**, p. 1042 (1968).
22) L. J. Cutrona, E. N. Leith, L. J. Porcello and W. E. Vivian: "On the application of coherent optical processing techniques to synthetic-aperture radar", Proc. IEEE, **54**, p. 1026 (1966).
23) H. F. Stockmann and B. Zarwyn: "Optical film sensors for RF holography", Proc. IEEE, **56**, p. 763 (1968).
24) D. Gabor: "A new microscopic principle", Nature, **161**, p. 777 (1948).
25) W. T. Gathey, Jr.: "The effect of finite sampling in holography", Optik, **27**, p. 317 (1968).
26) E. N. Leith and J. Upatnieks: "Reconstructed wavefronts and communication theory", J. Opt. Soc. Am., **52**, p. 1123 (1962).

27) E. N. Leith and J. Upatnieks: "Wavefront reconstruction with diffused illumination and three-dimensional objects", J. Opt. Soc. Am., **54**, p. 1295, (1964).
28) O. Bryngdahl and A. Lohmann: "Nonlinear effects in holography", J. Opt. Soc. Am., **58**, p. 1325 (1968).
29) J. W. Goodman: "Effects of film nonlinearities on wavefront-reconstruction images of diffuse objects", J. Opt. Soc. Am., **58**. p. 1276 (1968).
30) J. D. Armitage and A. W. Lohmann: "Theta modulation in optics", Appl. Opt., **4**, p. 399 (1965).